UNIVERSITÉ DE MONTRÉAL

THREE-DIMENSIONAL DECOMPOSITION OF GROUND-REACTION FORCES UNDER

BOTH FEET DURING GAIT USING PARAMETRIC CURVE MODELING

BAHARE SAMADI

INSTITUT DE GÉNIE BIOMÉDICAL

ÉCOLE POLYTECHNIQUE DE MONTRÉAL

MÉMOIRE PRÉSENTÉ EN VUE DE L'OBTENTION

DU DIPLÔME DE MAÎTRISE ÈS SCIENCES APPLIQUÉES

(GÉNIE BIOMÉDICAL)

AOÛT 2016

UNIVERSITÉ DE MONTRÉAL

ÉCOLE POLYTECHNIQUE DE MONTRÉAL

Ce mémoire intitulé:

THREE-DIMENSIONAL DECOMPOSITION OF GROUND-REACTION FORCES UNDER
BOTH FEET DURING GAIT USING PARAMETRIC CURVE MODELING

présenté par: SAMADI Bahare

en vue de l'obtention du diplôme de : Maîtrise ès sciences appliquées

a été dûment accepté par le jury d'examen constitué de :

M. BALAZINSKI Marek, Docteur ès sciences, président

M. RAISON Maxime, Doctorat, membre et directeur de recherche

M. ACHICHE Sofiane, Ph. D., membre et codirecteur de recherche

M. BALLAZ Laurent, Ph. D., membre et codirecteur de recherche

Mme PÉRIÉ-CURNIER Delphine, Doctorat, membre

DEDICATION

"Don't ever give up.

Don't ever give in.

Don't ever stop trying.

Don't ever sell out.

And if you find yourself succumbing to one of the above for a brief moment,

pick yourself up, brush yourself off, whisper a prayer, and start where you left off.

But never, ever, ever give up."

Richelle E. Goodrich

ACKNOWLEDGEMENTS

RÉSUMÉ

Introduction: La mesure tridimensionnelle des forces de réaction au sol (FRS-3D) est un élément important de l'analyse de la démarche. En effet, lors de l'évaluation fonctionnelle des patients en réadaptation, cette mesure permet de calculer les centres de pression, les paramètres spatio-temporels ainsi que les couples articulaires. Pour obtenir les FRS-3D sur plusieurs cycles de marche, l'utilisation de longues plateformes est nécessaire. Cependant, les systèmes de mesure de ce type posent un problème puisqu'ils fournissent uniquement une résultante des FRS-3D pour les deux pieds combinés. En plus, aucune méthode n'a précédemment été validée sur un nombre raisonnablement élevé de participants.

Objectif: Cette étude vise à développer une méthode automatisée en utilisant des courbes paramétriques en forme de « S » pour augmenter la précision de la décomposition des FRS-3D pendant les phases de double-appui, aux profils gauche et droit et ceci, le long des axes tridimensionnels X, Y et Z.

Méthodes: Trente adultes en bonne santé, âgés en moyenne de 24.8 ans (écart-type (ÉT) : 3.1 ans), dont 17 hommes, et ayant en moyenne un poids de 70.6 kg (ÉT : 11.4), ont marché naturellement, à pieds-nus, sur un plancher équipé de plateformes de force séparées. La méthode de modélisation de la décomposition de forces a été appliquée aux FRS-3D en considérant différentes fonctions paramétriques telles qu'une fonction polynomiale du $3^{\text{ième}}$ ordre, une sinusoïde et des sinusoïdes sigmoïdes. Pour valider cette méthode, les valeurs de FRS-3D décomposées ont été comparées à celles des FRS-3D enregistrées par plateformes de forces indépendantes et ceci pour chacun des sujets de l'étude. Une erreur globale est calculée en comparant la norme des valeurs de FRS-3D décomposées à celle de FRS-3D enregistrées par les

plateformes de forces indépendantes. Notons que la norme globale des FRS-3D est calculée par la moyenne quadratique des valeurs de FRS-3D le long de chaque axe.

Résultats: Pour les 30 sujets à l'étude, la plus faible erreur moyenne relative entre les FRS-3D globales calculées et celles enregistrées par plateformes de forces indépendantes étaient de 2.9% (ÉT :1.6%) en appliquant la fonction sinusoïde pour la force verticale (V), de 6.6% (ÉT :4.4%) en employant la fonction sinusoïde sigmoïde pour la force antéro-postérieure (AP) et de 9.5% (ÉT :3.6%) en décomposant par la fonction sinusoïde sigmoïde la force médio-latérale (ML), générant une erreur globale calculée de 3.2% (ÉT : 1.9%) sur les FRS-3D.

Discussion: Cette étude a proposé une méthode automatisée pour la décomposition des FRS-3D lors de la marche, qui utilise des paramètres cinétiques, et qui a été validée sur 30 sujets. Cette méthode peut être mise en œuvre pour obtenir la FRS-3D en temps réel (0.4, 0.8, 0.9 microsecondes pour V, AP, ML respectivement pendant la phase de double-appui) sur plusieurs cycles de marche sur les grandes plateformes. Cette méthode pourrait être étendue à l'analyse de divers mouvements comme la course, la danse, la marche avec un support ainsi que pour les études de réhabilitation.

ABSTRACT

Introduction: Three-dimensional ground reaction forces (3D-GRF) measurement is an important aspect of gait analysis to compute centers of pressure, spatial-temporal parameters and joint torques for functional evaluation in rehabilitation. To obtain these 3D-GRF on several gait cycles, a long measurement platform is required. However, the difficulty of such measurement systems arise from the fact that the unique force platform provides the resultant of GRF for the two feet combined. Therefore, one needs to decompose the 3D-GRF into components under each foot. Indeed, both feet are placed on the same force platform, which solely provides the global resultant of left and right foot together. Furthermore, no method has been previously validated on reasonable number of participants.

Objective: This study aims to develop an automatic method using s-type parametric curve modeling to increase the accuracy of decomposition of 3D-GRF during double stance into left and right profiles and along X, Y and Z axes.

Methods: Thirty healthy adults (age: 24.8 (Standard Deviation (SD): 3.1) years, 17 males, weight: 70.6 (SD: 11.4) kg) walked naturally barefoot on a floor equipped with separate force platforms. The decomposition modeling method was applied to global 3D-GRF using different parametric curve functions as in 3rd order polynomial, sine and sine-sigmoid functions. To validate this method, the decomposed 3D-GRF was compared to the 3D-GRF independently recorded for each subject. A global error is calculated based on global GRF, which is the comparison between the decomposed global 3D-GRF and recorded global 3D-GRF. The global 3D-GRF is obtained by computing the square root of the sum of the second exponential of GRF along each axis.

Results: For the 30 subjects, the relative average errors between the decomposed GRF by best function and the 3D-GRF independently recorded by force platforms were equal to 2.9% (SD: 1.6%) decomposed by sine function for the vertical forces, 6.6% (SD: 4.4%) decomposed by sine-sigmoid function for the antero-posterior forces and 9.5% (SD: 3.6%) decomposed by sine-sigmoid function and for the Medio-lateral forces, providing a global error on global forces of 3.2% (SD: 1.9%) on the 3D-GRF.

Discussion: This study proposed an automatic method for 3D-GRF decomposition during gait analysis using kinetics parameters and was tested on 30 subjects. The method can be implemented to obtain the 3D-GRF in real-time (0.4, 0.8, 0.9 microseconds for V, AP, ML respectively during one double stance phase) for several gait cycles on long platforms and could be extended to various movement analyses such as running, dancing, walking with a support and for rehabilitation studies.

TABLE OF CONTENTS

LIST OF TABLES

LIST OF FIGURES

LIST OF SYMBOLS AND ABBREVIATIONS

3D	Three-dimensional
AP	Antero-posterior ground reaction force
BM	Body mass
COP	Centre of pressure
DS	Double stance phase of gait cycle
GRF	Ground reaction forces
ML	Medio-lateral ground reaction force
SD	Standard deviation
SS	Single stance phase
V	Vertical

CHAPTER 1   INTRODUCTION

Nowadays studies on gait analysis cover a wide range of interests and domains; i.e. clinical purposes in terms of computing centers of pressure, spatial-temporal parameters, joint torques, movements recognition and health monitoring [1], [2] and civil engineering in terms of understanding the interactions between the foot, the structure and the dynamical behavior of the structure underneath it [3]. These interests lead to the need of recording ground reaction forces (GRF) during gait.

For this purpose, separate force platforms, long force platforms and treadmills equipped with force platforms are generally used. However, there are some advantages and disadvantages in using both of them. Using the single platforms provides the possibility of directly having GRF under each foot; meanwhile it may lead to the need of performing numerous gait trials to obtain valid cycles, where both steps are fully inside the force platforms. Furthermore, even when the 3D-GRF is obtained they can be a result of undesirable targeted steps. In fact the participants might unconsciously change their gait patterns in terms of targeting their steps to hit the separate platforms and therefore altering their natural gait pattern and the 3D-GRF values [4], [5].

 In gait studies, there are always attempts to avoid long evaluation time and targeted footsteps. This may have undesirable impact on the results of studies concerning muscular fatigue contents as well as individuals with impaired gait and children [6]. Thus, it might be possible to reduce the number of trials by arranging starting positions of each subject to make the stances coincide with the force platforms [7]. It has been reported that changing only 10% in step length has a significant impact on GRF [5], [7], [8].By using unique force platforms, obtaining the desired cycles is not complicated but the recorded GRF represent the total forces under both feet. To have better understanding of gait pattern and GRF during walking in individuals, it is needed to have GRF separately under each foot.

The gait cycle is composed of 60% of stance phase when foot is in contact with the ground and 40% of swing phase where foot is in the air [9]. The stance phase includes the single stance phase when there is one foot in contact with the ground and the double stance phase when both feet are in contact with the ground. The need for decompose GRF is obviously needed during DS, which is about 25% of each gait cycle (Figure 1.1).
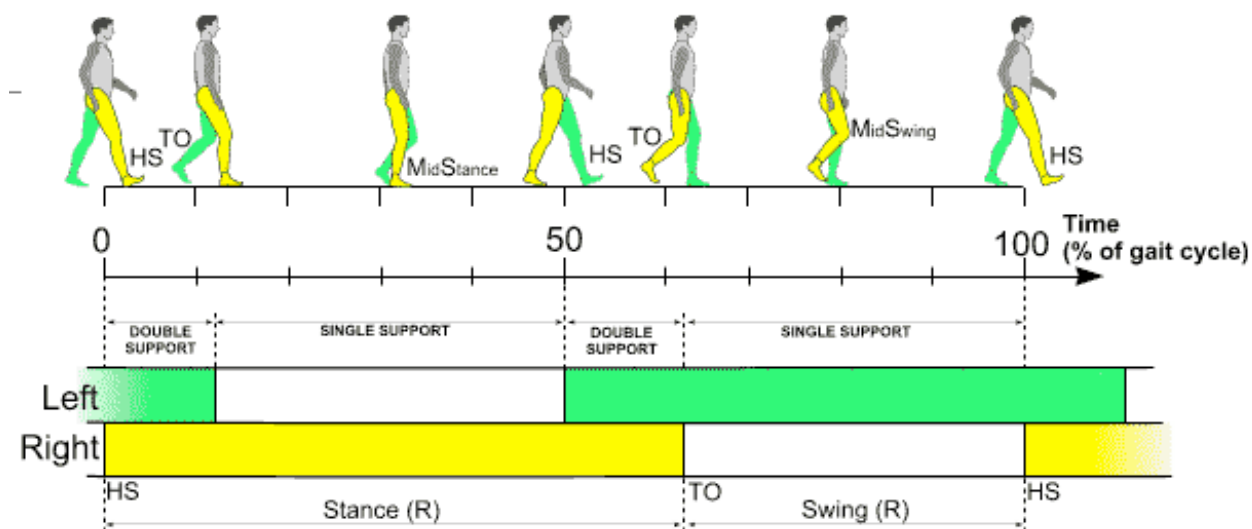
Figure 1.1: Gait cycle phases [10]

The decomposition methods are usually based on kinetics and kinematics variables of SS before and after DS as well as gait velocity. Kinematics parameters during gait are referred to the human joints and segments movements independent of forces, which are recorded by motion capture systems. They include displacements, velocities and accelerations that happen in the articulations during gait. Kinetics parameters are the forces that cause human movements. It is composed of internal and external forces. The source of internal forces is muscle activity or the friction in the muscles and joints, and the external forces come from the ground or external loads [11].

Although some methods have been proposed to decompose 3D-GRF, to the author's knowledge, they mainly use, kinematics parameters and gait speed. However, the kinetics parameters have better predictability than the kinematics parameters with gait speed [12].

Consequently, this thesis aims to propose an automatic s-type parametric curve-fitting model to decompose 3D-GRF along the three axes (X, Y, Z) under left and right profiles. This method can be applied without the need of a motion capture system by using kinetics parameters of the single stance phase before the double stance phase.

The main characteristic needed for the method proposed in this thesis is to be easily implemented in various populations and domains such as functional evaluation in rehabilitation [1]. Indeed, in clinical populations including children and adults, the gait analysis play an important role in their pre-treatment assessment, surgical decision making and postoperative follow-up[13].

The rest of this document is organized as following. In chapter 2, state-of-the-art is presented. The objective of this master project is discussed in chapter 3. Chapter 4 is an article that was submitted to report the final results of this project. Chapter 5 thoroughly explains the methodology. The results of the study is demonstrated in chapter 6. A discussion over the results of this project is presented in chapter 7; and chapter 8 is the conclusion and recommendations of possible implementations concerning the motion analysis.

CHAPTER 2   LITERATURE REVIEW

Research works related to ground reaction forces decomposition can be divided into two main categories: 1.Studies concerning detection of gait events, which are the transition between single stance phase (SS) and double stance phase (DS); and 2.Studies concerning decomposition ground reaction forces (GRF) itself. However, to decompose GRF, it remains essential to detect phase transition. In this chapter, first we present a comprehensive literature review on these two main categories and then explain the problem of this research project.

2.1 Studies on determination of gait events

Begg (2000) [14] proposed a method to detect the transition between SS and DS, assuming that a local minimum is present in GRF patterns before and after each DS. This assumption is the major limitation of applying this method, since minima are not systematically present in natural GRF patterns [7].

O'Connor *et al.* (2006) [15] detected the transition between SS and DS automatically based on a simple velocity curve derived from heel and toe marker trajectories, using a motion capture system.

Zeni *et al.* (2008) [16] proposed two automatic algorithms using solely kinematics data to detect gait events. Both of the algorithms were based on the positional changes of the foot markers.

The major problem of these two studies is the need for a motion capture system.

2.2 Studies on GRF decomposition

Davis and Cavanagh (1993) proposed a method to decompose vertical (V) GRF under each foot using a unique large force platform [8]. Their method was based on examining side-to-side oscillations of the measured center of pressure (COP), and detecting the phase transition when the COP exceeds a certain threshold. They calculated the individual GRF profiles by means of solving two simultaneous equations. One equation defined the equilibrium of forces in the vertical direction, and the other one defined the equilibrium of moments about an antero-posterior axis of the force platform. Although their study was the most cited on decomposing V GRF [17]–[21], some uncertainties exist in their proposed method. For example, the detection of phases on the basis of examining side-to-side oscillations of the global COP may not be an accurate method

for children due to their lower weight or subjects with impaired gait, since the oscillations of the global COP may not be performed properly. However, in numerous cases, the COP path of Medio-lateral (ML) forces does not systematically show a clear side-to-side inflection point as presented by Davis and Cavanagh. The robustness of the method has not been largely tested on different participants with diverse gait patterns. They validated their method on one healthy adult only, walking with three different speeds (Figure 2.1) [8].
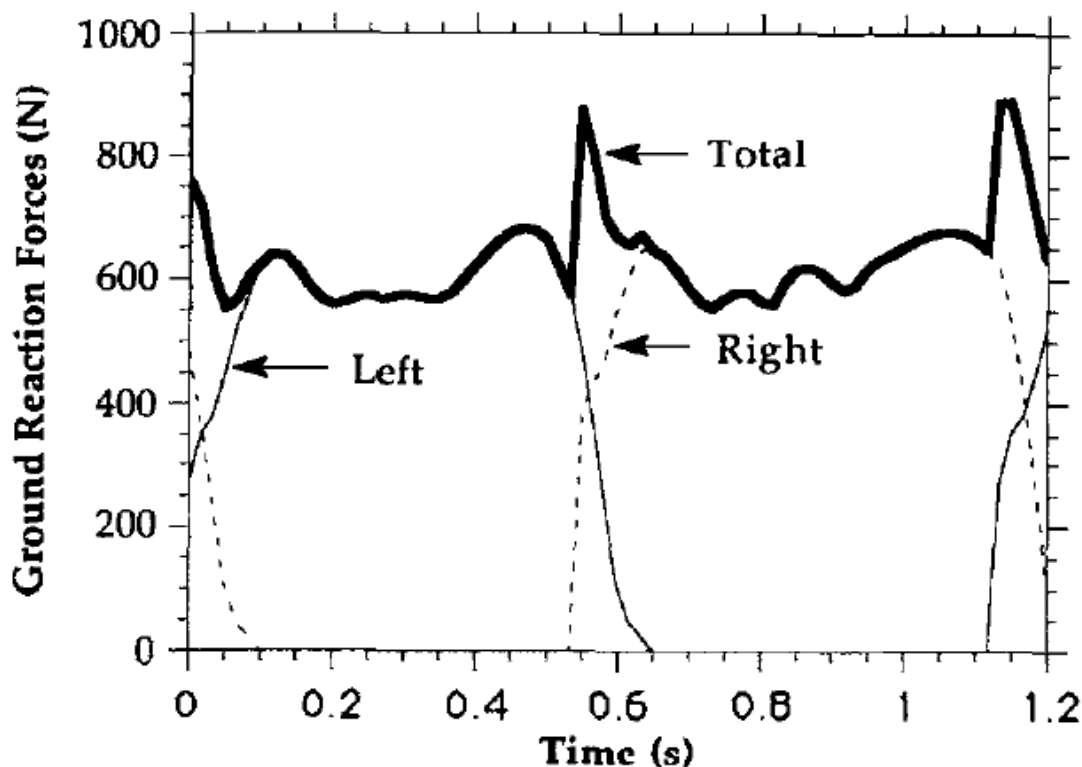
Figure 2.1: Temporal summation of left and right GRF profiles for successive steps [8].

Ballaz *et al.* (2013) [7] (a study from our laboratory) developed the first automatic method to detect the SS and DS transition using difference of COP in the horizontal plane between two given time instants. They also proposed the first automatic method to decompose the V GRF profiles during the DS by using cubic spline curve interpolation. In a cubic spline interpolation, a series of cubic polynomials are fitted between the first and the last points of the DS, while the obtained curve is continuous and smoothed [22]. The proposed decomposition method was based on predicting GRF applying cubic spline curve interpolation by modeling the curve of the first

foot leaving the ground (Figure 2.2). The foot that first leaves the ground has a smoother curve compared to the second foot.

Therefore the decomposed GRF of the second foot was obtained by differentiating between the total force and the decomposed force of the first foot leaving the ground. The mean relative error for V GRF was 3.8%. They validated their method on 6 typically developed children performing a total of 36 stances. However, the decomposition of the other components of GRF i.e. ML and antero-posterior (AP) were not studied. Whereas the interpolation method is less suitable for clinical gait, since the transition is not always smooth [21].
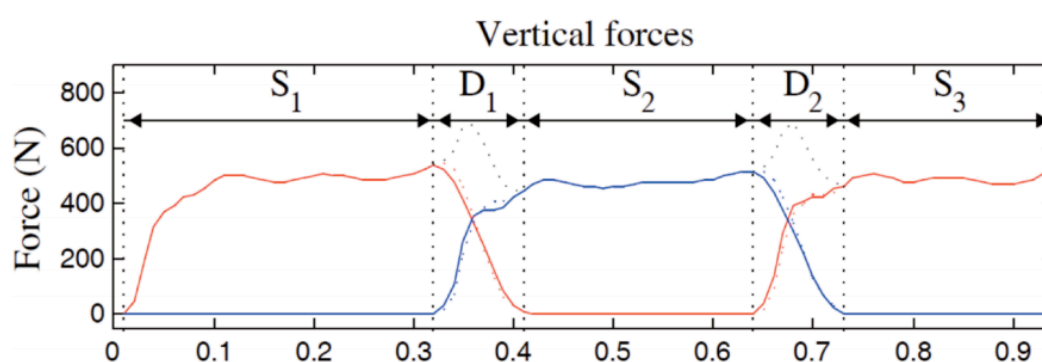
Figure 2.2: Time evolution of the vertical components of the GRFs approximated by splines (solid line) and the corresponding measured GRFs (dotted line); the total measured vertical GRFs are also presented in dotted lines during the double stances [7]

Oh *et al.* (2013) [23] predicted forces and moments during SS and DS. They applied a genetic algorithm-general regression neural network; using 14 kinematics parameters of gait during SS. They used the experimental data of the 43 subjects as training data and validated their method on 5 healthy adults (Figure 2.3). The mean relative errors were up to 11.7%. The major practical limitation of their method to compute GRF was as this method would require a motion capture system and a training process when the targeted population is changed.

Ground Reaction Forces (N/kg)
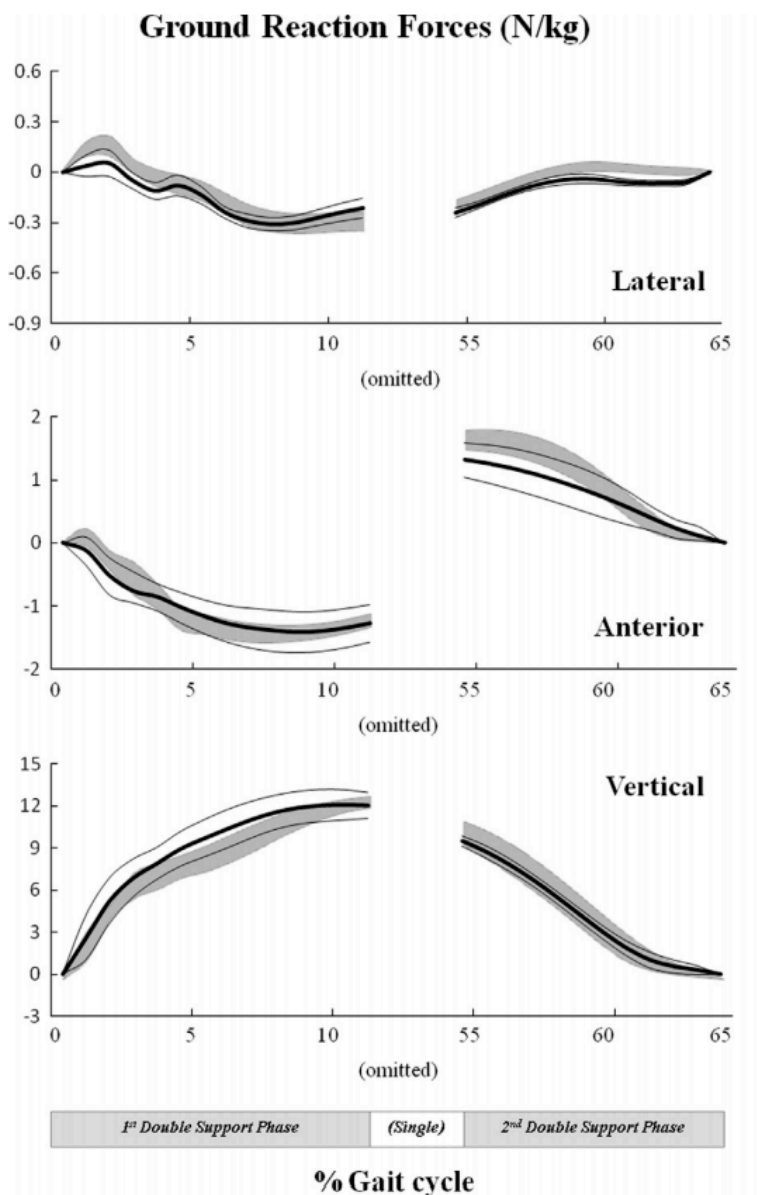
Figure 2.3: Predicted GRF from the artificial neural network method (mean (thick line) ± 1 SD (thin lines), described as the mean of 10 folds) vs. measured GRF (mean ± 1 SD (shaded area)) in the double support phase [23]

Villeger et al. (2014) [24] succeeded to propose a method in decomposing the 3D-GRF with mean relative error up to 18.01%. In their proposed method, a shape coefficient was adjusted using GRF kinematic parameters, including the gait velocity, during single stance phase. This coefficient was optimized by a non-linear least-square curve fitting to fit the predicted signals

with the recorded GRF. Then the GRF were decomposed to left and right profiles performing a multiple regression (Figure 2.4). But again the same limitation, which is the need of motion capture system, exists.
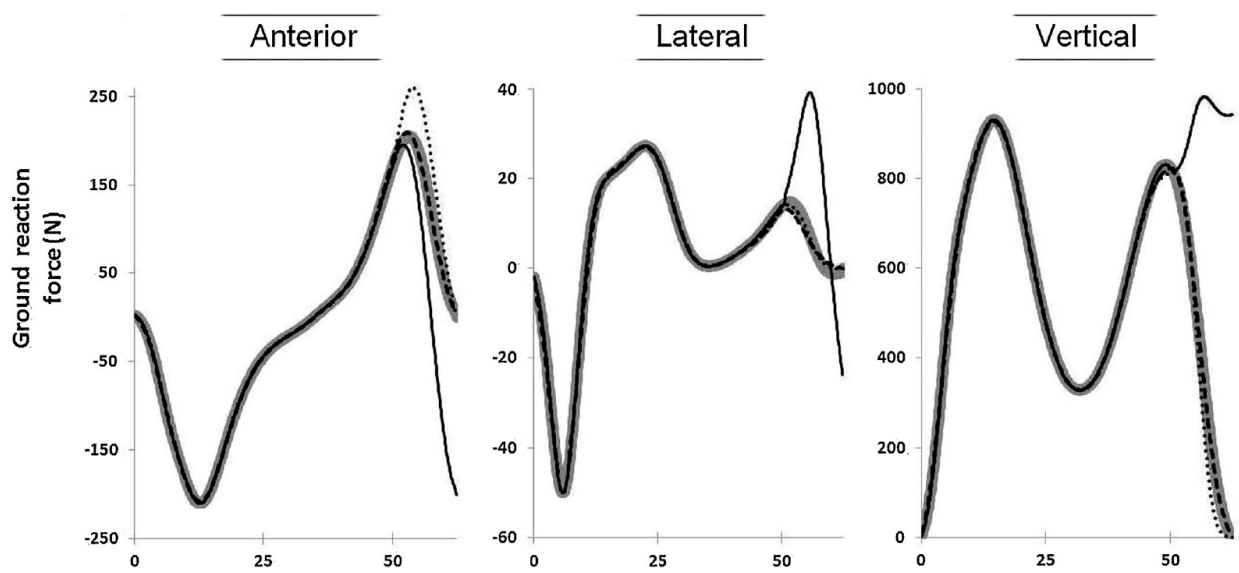
Figure 2.4: Illustration of total GRF (black line), real GRF (large gray line), GRF from our method (black dashed line) and GRF from Ren's method (black pointed line) for the foot leaving the ground [24].

Meurisse *et al.* (2015) [21] proposed a method to determine GRF based on the distance covered by COP. The developed algorithm was a revision of Davis and Cavanagh method [8]. However they validated their method on V GRF only and not on 3D-GRF.

Hijazi and Makssoud (2015) [25] proposed a hyperbolic tangent function to decompose V GRF by defining the parameters of the function. The parameters were determined by iterations on a compatible computer using MATLAB® (Mathworks®, USA). They obtained the function parameters by minimizing the sum of the squared parameters. Marquardt parameter [26] was considered as initial value of the parameters. The iteration procedure was defined to stop at 10^{-7} for the residual sum of square. They tested their proposed method on one healthy adult walking with three different gait velocity. However, the method was not validated by comparing recorded GRF and decomposed GRF (Figure 2-5). Therefore the accuracy of their proposed model is

questionable. In addition the number of iterations for each parameter vary from 72 to 151 which can be considered as a long time procedure.
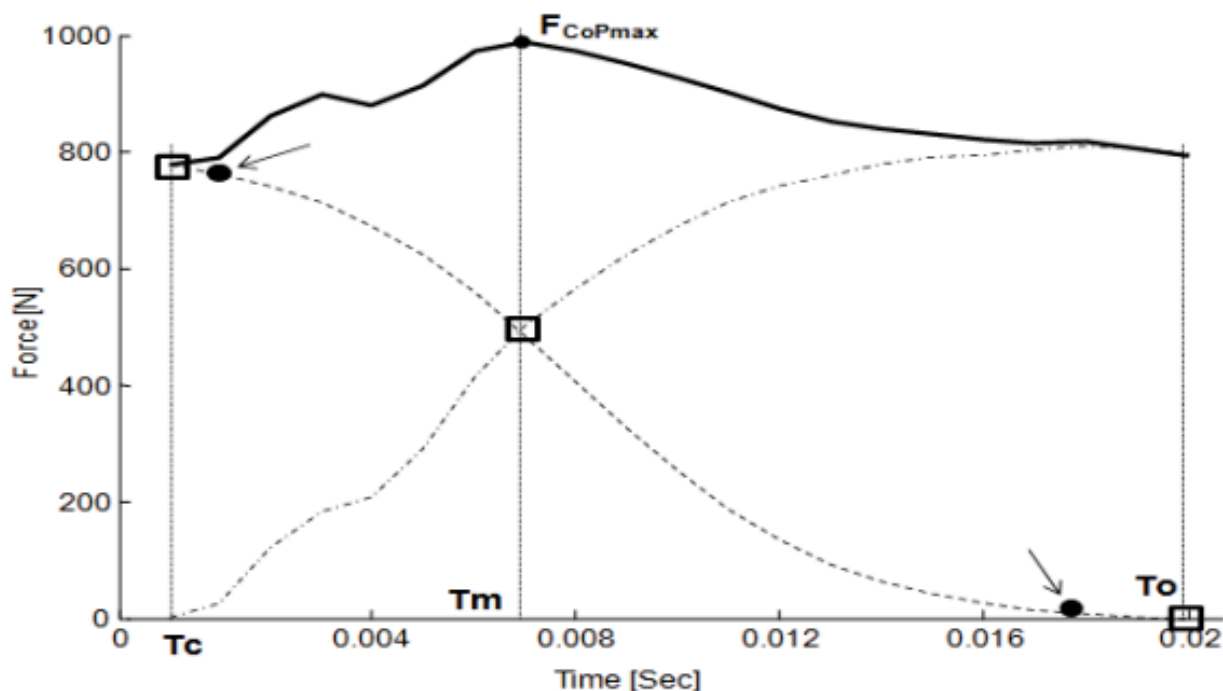
Figure 2.5: Right (dashed), left (dot-dashed) GRF and the sum during double stance phase (line). T_C, T_M and T_O (Instants T_C, T_M and T_O correspond to the detected FC (foot contact), maxima F_{CoP} (center of pressure) and FO (foot off) gait events respectively) correspond to the detected FC, maxima F_{CoP} and FO gait events respectively. Arrows mark the additional points for improvements [25].

2.3 Problem

As cited above, the major limitation of the methods used for the decomposition of 3D-GRF, is the need for a motion capture system [23], [24]. Furthermore, most of the studies concerning GRF focus on the decomposition of V GRF only [7], [8], [21], [25] and ignore the other two axes. The geometric curve pattern of ML and AP GRF are more variable during gait in comparison to the vertical GRF. This variability can be explained due to the small magnitudes of ML and AP GRF, in comparison to the V GRF [27]. Therefore applying decomposition methods on ML and AP

GRF are more complex than for V GRF. Some others studies focus on the detection of gait events (DS and SS) and not decomposing 3D-GRF [15], [16], [28]–[30] . Due to the fact that GRF decomposition methods are applied only during DS, it is essential to detect the transition between phases while using long single force platforms in gait analysis. Furthermore, the number of participants in most of the above-mentioned research works, was generally quite low, ranging from one single participant to 7 participants; whereas the current research project used 30 healthy subjects, and can be implemented without the need of a motion capture system.

The general geometric curve pattern of GRF during double stance phase presented in [7], [21], [23]–[25], [31] and the recorded experimental data of this research project (Figures 2.1-2.3) showed the similarity between the profiles of the GRF and s-type functions. s-type functions are referred to the mathematical functions that produce s-type shapes [32]. This is the reason why we chose to use different types of s-type functions to compute GRF during DS.
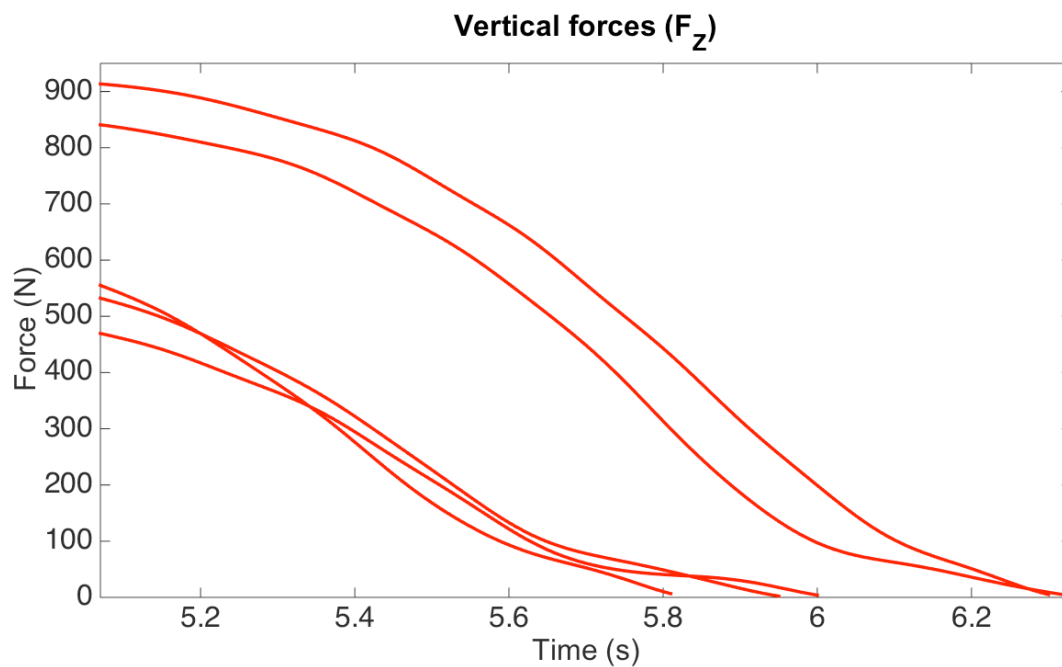
Figure 2.6: Recorded vertical GRF during double stance phase of 5 different individuals

Antero-Posterior forces (F$_Y$)
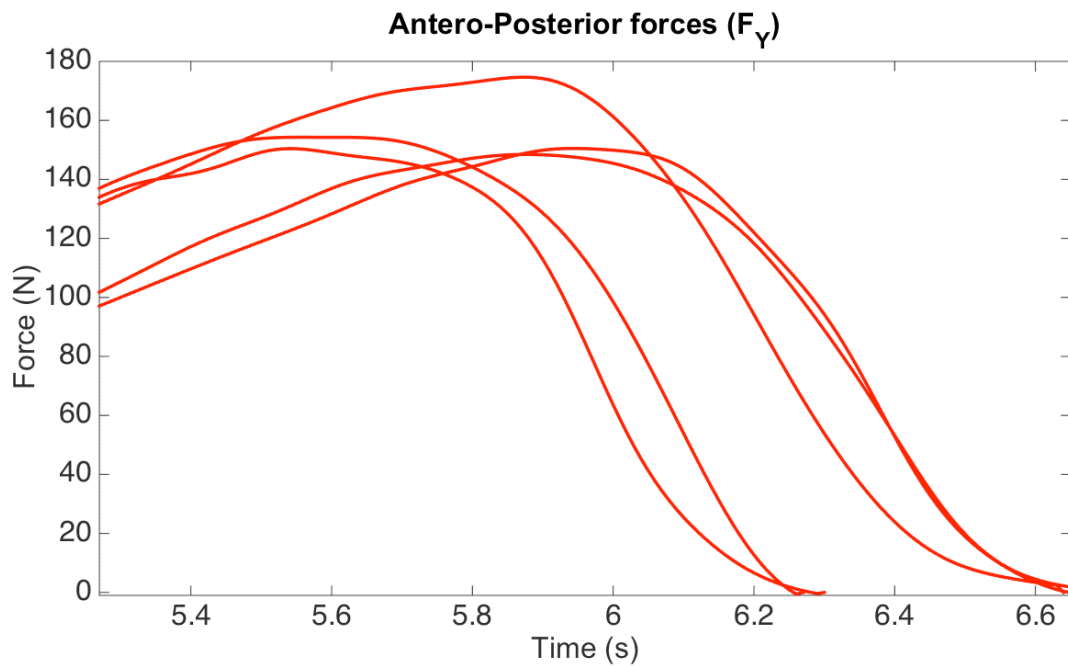
Figure 2.7: Recorded antero-posterior GRF during double stance phase of 5 different individuals

Medio-Lateral forces (F$_X$)
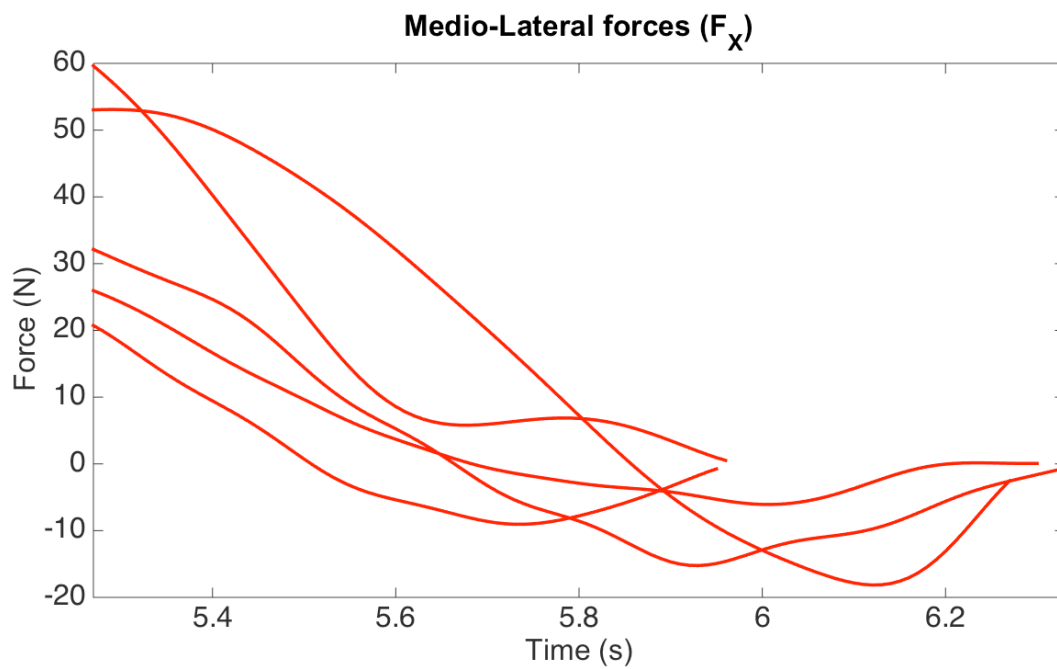
Figure 2.8: Recorded medio-lateral GRF during double stance phase of 5 different individuals

2.4 Summary of the problem

The literature review has identified the followings:

- There is not any report study on decomposing 3D-GRF that does not use a motion capture system.

- The proposed methods have not been widely tested on a large sample of participants.

CHAPTER 3   RATIONALE OF THE PROJECT

3.1   General objective

The general objective of this project is to develop a method to increase the accuracy of decomposition of 3D-GRFs under each foot and along X, Y and Z axes using s-type parametric curve modeling.

3.2   Specific objective

The specific objective of this project is   defining the best s-type function.

3.3   Hypothesis

The research hypothesis of this project is by using s-type parametric curves using gait information from SS will yield more accurate results than the literature for predicting GRF along X, Y and Z axes.

3.4   Research questions

The main research question of this project is:

How to decompose GRF during DS applying s-type parametric curve fitting models without using a motion capture system?

The complementary research questions are:

- What are the mathematical functions the most suited for modeling 3D-GRF?

- Is there one unique function that can model the 3D-GRF with minimal errors along X, Y and Z axes?

- Does the hypothesis lead to better results than the results using spline interpolation method?

CHAPTER 4 ARTICLE 1: "DECOMPOSITION OF THREE-DIMENSIONAL GROUND-REACTION FORCES UNDER BOTH FEET DURING GAIT USING PARAMETRIC CURVE MODELING"

4.1 Presentation of the article

DECOMPOSITION OF THREE-DIMENSIONAL GROUND-REACTION FORCES UNDER BOTH FEET DURING GAIT USING PARAMETRIC CURVE MODELING

The following article was submitted on July 2016. This article presented the results of this master research project, submitted to 'Gait and Posture journal'.

As first author, the M.Sc. candidate has 75% of contribution.

"Decomposition of three-dimensional ground-reaction forces under both feet during gait using parametric curve modeling"

Bahare Samadi [a,b*], Sofiane Achiche [c], Laurent Ballaz [b,d], Maxime Raison [a,b,c]

[a] *Rehabilitation Engineering Chair Applied to Pediatrics, Polytechnique Montréal and Sainte-Justine UHC, Montreal (Qc), Canada*

[b] *Research Center – Sainte-Justine UHC, Montreal (Qc), Canada*

[c] *Department of mechanical engineering, Polytechnique Montréal, Montreal (Qc), Canada*

[d] *Department of physical exercise sciences, Université du Québec à Montréal (UQAM), Montreal (Qc), Canada*

[*] Corresponding author:

Bahare Samadi

Rehabilitation Engineering Chair Applied to Pediatrics (RECAP),

Polytechnique Montréal, Principal building, room A530,

2500, Chemin de Polytechnique

Montreal, Quebec

Canada H3T 1J4

Tél. : +1 (514) 340-4711 # 3345

Email address: bahare.samadi@polymtl.ca

Conflict of interest: None

4.2 Abstract

Introduction: Obtaining the three-dimensional ground reaction forces (3D-GRF) requires a platform path, such as a long platform or several juxtaposed platforms. The main shortcoming of these platform paths is that during double stance phases of gait, both feet can be placed on the same force platform causing the need for decomposing the 3D-GRF into left-foot and right-foot profiles. **Objective:** The current study presents an automatic method using s-type parametric curve modeling to increase the accuracy of decomposition of 3D-GRF during double stances under each foot, along X, Y, and Z axes. **Methods:** Thirty healthy adults walked naturally on a floor equipped with separate force platforms. The decomposition method was applied to the global 3D-GRF using 3rd order polynomial, sine, and sine-sigmoid functions. The computed 3D-GRF was compared to the 3D-GRF independently recorded by force platforms for each subject. **Results:** The relative average error between the computed 3D-GRF and the recorded 3D-GRF were equal 3.2±1.9%. In details for the vertical, antero-posterior, and medio-lateral forces, these errors were 2.9±1.6%, 6.6±4.4%, and, 9.5±3.6%, respectively. The computation times were up to 0.9 ms during one double stance phase in MATLAB$^{®}$. **Discussion and conclusion:** This study proposed an automatic 3D-GRF decomposition method, tested on 30 subjects. The global error on the GRF is the best one in the literature. The process works in real-time, enabling to be implemented on platform paths. The perspectives are to validate the method for various populations with musculo-skeletal disorders, extend it to various movement analyses, and compute the corresponding spatio-temporal parameters without the use of any motion capture system.

Keywords: gait; prediction of 3D ground reaction force; force platforms; double stance phase decomposition; s-type parametric curve modeling

Abbreviations:

3D: Three-dimensional

AP: Antero-posterior

COP: Centre of pressure

DS: Double stance

GRF: Ground reaction forces

ML: Medio-lateral

SD: Standard deviation

SS1: Single stance phase before the double stance phase

SS2: Single stance phase after the double stance phase

V: Vertical

4.3 Introduction

Ground reaction forces (GRF) under each foot are crucial to different domains ranging from biomechanics, to compute centers of pressure and spatio-temporal parameters [1–3], health monitoring [4,5] and structural dynamics, to model the interaction between the foot and the structure [1,6].

Three-dimensional ground reaction forces (3D-GRF) are traditionally recorded using separate platforms under each foot, but it may lead to a large number of trials to get a valid cycle i.e. both steps inside the force platforms separately, which is both time consuming and difficult to achieve [7]. In fact, the participants might unconsciously change their gait patterns in terms of targeting their steps to hit the separate platforms and therefore altering their natural gait pattern and consequently the 3D-GRF [7]. Changing only 10% in step length has a significant impact on GRF [8–10]. Moreover, increasing the number of trials leads to muscular fatigue and can hence also affect the results [11,12].

Therefore, the interest in using other means such as single long force platforms and force measuring shoes and insoles has emerged as substitute solutions for more accurate gait analysis. Measuring shoes and insoles, can only be used for measuring vertical forces and pressures, which is not a reliable clinical measure of 3D-GRF solely due to its sensitivity to any action or reaction changing the ground reaction force vector [13,14].

Consequently using unique force platforms emerges as a practical method to facilitate and accelerate the procedure of recording GRF data for a varied population [15]. The remaining challenge is to decompose the global 3D-GRF under each foot, since the long force platform only provides the resultant of GRF for the two feet combined.

Decomposing the GRF has been a challenge for more than two decades. First Davis and Cavanagh (1993), proposed a method to decompose vertical GRF profiles [8]. They validated their method on only one healthy adult walking with three different speeds. To detect the transition between phases, their proposed method was based on the analysis of the side-to-side oscillations of the global center of pressure (COP). In numerous cases, the COP path of medio-lateral forces does not systematically show a clear side-to-side inflection point [9]. Meurisse et al.

(2015) [16], developed their method based on Davis and Cavanagh idea, but only to decompose vertical GRF.

Ballaz et al. (2013) were the first authors to propose an automatic method to detect SS and DS transition based on the difference of COP in the horizontal plane between two given time instants. They also proposed an automatic method to decompose vertical GRF profiles by using interpolation splines with an average error of 3.8%, tested on 6 typically developed children [9,17]. However spline interpolations do not consider the typical patterns of GRF which are not always smooth, therefore potentially leads to inaccuracies [16].

Hijazi and Makssoud (2015) [18] proposed a method tested on one healthy adult, using a model based on hyperbolic tangent function to decompose vertical (V) GRF. The robustness of the method can be questionable since they did not validate their method by comparing the computed GRF to the recorded GRF. However, their model was sensitive to the quality of initial values of parameters.

The studies discussed above could not achieve to decompose GRF along the two other axes, which are antero-posterior (AP) and medio-lateral (ML) axes. However, they remain essential to 3D-GRF decomposition, since they are recognized as more variable force indicators than the V GRF [19]. It can be explained by their relative small magnitudes in comparison to the vertical forces [20].

Recently, Oh et al. (2013) [21] and Villeger et al. (2014) [22] decomposed 3D-GRF by applying genetic algorithm-general regression neural network and multiple regression parameter models, respectively. The major practical limitation to compute GRF in these methods is the need for motion capture systems.

Some studies have been also performed only to detect the transition of the phases using motion capture systems [23–26].

Consequently as of today, no method has been proposed for the decomposition of 3D-GRF solely using force platform measurements. Furthermore, no method has ever been tested on at least 30 subjects to enable large group statistics.

The aim of this study is to develop an automatic method that decomposes global 3D-GRF under each foot during the DS by using s-type parametric curve modeling. This method would be

suitable for any platform path, whether a long force platform or juxtaposed platforms, and without need of a motion capture system.

4.4 Methods

4.4.1 Participants

Thirty healthy adults volunteered for this study with an average age of 24.8 (standard deviation (SD): 3.09 year), range: 20-34; 17 male.

4.4.2 Set-up and procedure for data collection

The experimental procedure was explained for each participant and all participants provided written informed consent prior to test.

To record left and right GRF independently measured on two platforms during untargeted gait, the participants were asked to walk naturally barefoot at their own preferred speed, looking straight ahead without targeting their steps on the platforms. The trials with both steps inside the force platforms were systematically used for this study.

A low-pass filter with a 4th order Butterworth using a 4Hz cut-off frequency was applied to the GRF to remove the noise.

4.4.3 Computed parameters and GRF decomposition

To have a better understanding of the global approach used in this paper, the complete steps of the procedure are summarized in figure 4.1 and detailed in the following sub-sections.

$$\downarrow \Delta COP_{t,T}^2$$

Step 1: Detect the transition between single and double stance phases

↓ Transitions between SS and DS phases

Step 2: Observe the geometric of gait patterns during DS to select the appropriate functions with similar behavior to GRFs

↓ Choose preliminary S-type functions

Step 3: Choose the functions to be used in curve-fitting model based on step 2

↓ Apply appropriate functions to be used for computing GRF during DS using kinetic data during SS

Step 4: Compute 3D-GRF of first landed foot along with the X, Y and Z axes applying curve fitting model using chosen functions

↓ $F_{computed}$ of first landed foot

Step 5: Obtain computed GRF of the second landed foot

↓ $F_{computed}$ of second landed foot

Step 6: Calculate the errors for each 3D-GRF component and each axis

↓ Absolute error (e_F), relative error (ε_F)

Step 7: Choose the best fitted function for 3D-GRF along X, Y and Z axes

↓ AP (F_y) GRF→ Sine-Sigmoid function
ML (F_x) GRF→ Sine-Sigmoid function
V (F_z) GRF→ Sine function

Figure 4.1: Summary of methodology

DS: Double stance, SS: Single stance, 3D-GRF: Three dimensional ground reaction forces,: Computed GRF by proposed method,: Individually measured GRF on each platform during DS under each foot, : Total recorded GRF on the platforms,: GRF under the second landed foot, AP: Antero-posterior GRF, ML: Medio-lateral GRF, V: Vertical GRF

To detect the transition between SS and DS (step 1), first the center of pressure (COP) of each force platform was obtained and then the global COP was computed. The peak of (Eq. 1) was then compared with the constant thresholds to detect the phase transitions.

$$\Delta COP^2_{t,T} = \left(OP_{x_{t+T}} - OP_{x_t}\right)^2 - \left(OP_{y_{t+T}} - OP_{y_t}\right)^2 \tag{1}$$

where y axis is aligned with the AP, x axis is aligned with the ML ,and z axis is aligned with the V direction (Figure 4.2):

- OP is the vector of the local COP position for each platform;

- ΔCOP is squared Euclidian norm in the horizontal plane between two given time instants t and $t + T$ of the global center of pressure.
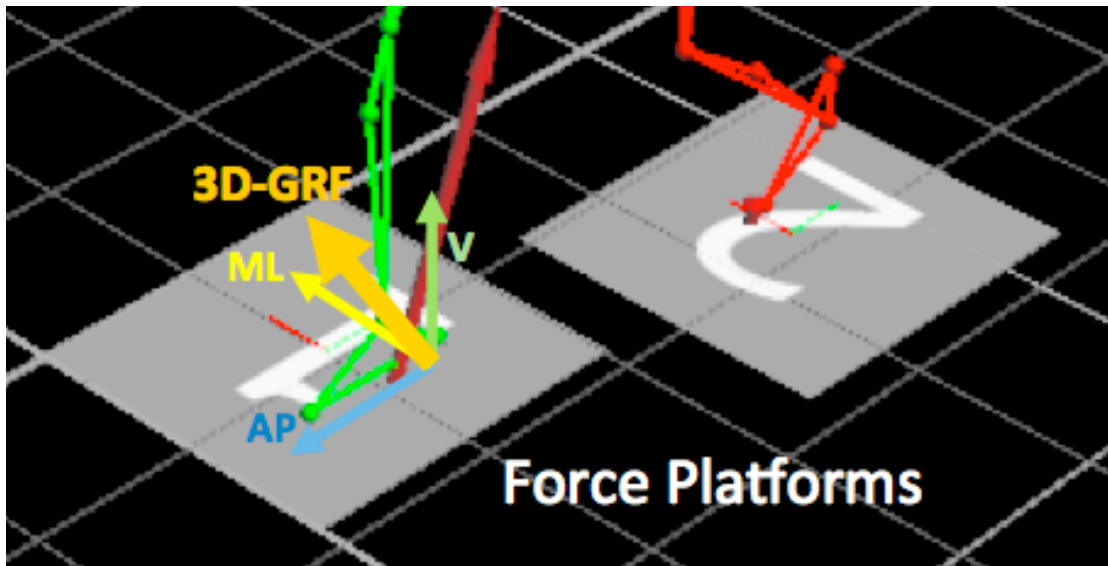
Figure 4.2: Focus on the human body walking on the force platforms.

V: Ground reaction forces (GRF) along with the vertical axis, ML: GRF along with the X axis, AP: GRF along with the Y axis, 3D-GRF: Global GRF (Eq. 22, 23), which is the norm of the V, AP and ML components of GRF.

A preliminary study was performed using a curve fitting method on the recorded GRF during DS to choose the best functions to fit to the GRF. For this purpose. MATLAB[®] (Mathworks, Natick, Massachusetts, U.S.A.) *lsqnonlin* curve fitting tool, which solves nonlinear data fitting problems was used. The initial values were specified by iteration.

Although some differences do occur due to different walking behavior [20] (Step 2), the observation showed that in average the best functions, fitted for GRF components during DS, were chosen as 3rd order polynomial, sine and sine-sigmoid as shown in the equations 2-5 respectively (Step 3).

$$f_{poly}(x) = A_{poly}x^3 + B_{poly}x^2 + C_{poly}x + D_{poly} \qquad (2)$$

$$f_{sine}(x) = A_{sine}\sin\left(\frac{x}{B_{sine}} - C_{sine}\right) + D_{sine} \qquad (3)$$

$$f_{sig}(x) = \frac{A_{sig}}{1 + e^{B_{sig}(x - C_{sig})}} \qquad (4)$$

$$f_{sine-sig}(x) = f_{sine}(x) + f_{sig}(x) \qquad (5)$$

where x is the time samples of experimentally recorded GRF during DS.

The GRF were computed by applying the selected functions (Step 4).

It is worth noting that in our proposed method to compute the parameters of each function, we do not need to solve any non-linear least square problems. We defined the parameters on the basis of the kinetic information during SS before the DS and the fact that the value of the force in the modeled foot is equal to zero as soon as it leaves the ground. However, we found the relation between the function parameters and forces and temporal information [18].

The following sub-sections present the computation of the parameters for the $f_{poly}(x)$, $f_{sine}(x)$, $f_{sig}(x)$, and $f_{sine-sig}(x)$ respectively.

4.4.3.1 Computation of the 3rd order polynomial function

To compute the GRF during DS using 3rd order polynomial function, the equations 6-9 are used (Figure 4.3a). These equations are defined using the kinetic parameters during SS1 provided by force platforms:

$$f_{poly}(x_0) = LFSS \tag{6}$$

$$f'_{poly}(x_0) = dFSS \tag{7}$$

$$f_{poly}(x_L) = 0 \tag{8}$$

$$f'_{poly}(x_L) = E \tag{9}$$

where:

- x_0 (1×1) is the last time of the first single stance phase (SS1) before the DS;

- $LFSS$ (1×1) is the value of GRF in the last frame of SS1;

- $dFSS$ (1×1) is the mean slope of GRF for the last 5 frames of SS1 (the last 5 frames were chosen to describe the slope tendency);

- x_L (1×1) is the first frame of second single stance (SS2) after DS where the first foot leaves the floor;

- E (1×1) is the slope of the GRF of the first landed foot, at the first frame of SS2, which is equal to 0.

4.4.3.2 Computation of the sine function

To compute the GRF during DS using sine function, the required parameters for sine function are calculated by the equations 10-13:

$$A_{sine} = a \times LFSS \tag{10}$$

$$B_{sine} = b \times t_{DS} \tag{11}$$

$$C_{sine} = (x_0 + c_1) - (c_2 \times t_{DS}) \tag{12}$$

$$D_{sine} = d \times LFSS \tag{13}$$

where:

- A_{sine} (1×1) is amplitude of sine function;

- $1/B_{sine}$ (1×1) is period of sine function;

- C_{sine} (1×1) is horizontal phase shift of sine function, defines the start point of sine function for each GRF in horizontal axis;

- D_{sine} (1×1) is vertical phase shift of sine function, defines where the computed curve should be started vertically;

- a (1×1) is a constant value that determines the appropriate codomain of sine function to adjust with the experimental GRF, which is equal to 0.6 for ML and AP GRF, and 0.5 for V GRF practically defined based on geometric pattern comparison between the experimental curve of GRF along each axis and a typical sine curve;

- $LFSS$ (1×1) is the value of GRF in the last frame of SS1 (Figure 4.3a);

- b (1×1) is a constant value determines the required period of the sine function adjusted to the experimental GRF which is equal to 2, practically defined based on geometric pattern comparison between the experimental curve of GRF along each axis and a typical sine curve;

- x_0 (1×1) is the last frame of SS1(Figure 4.3a);

- t_{DS} (vector, n×1) is the duration of DS phase;

- c_1 (1×1) is a constant value, determines the start point of sine function appropriate for GRF along each axis, which is equal to -20 for ML, +20 for AP, and 0 for V GRF, practically defined based on geometric pattern comparison between the experimental curve of GRF along each axis and a typical sine curve;

- c_2 (1×1) is a constant value to calculate the required horizontal phase shift, practically defined on the basis of geometric pattern comparison between the experimental curve of GRF along each axis and a typical sine curve which is equal to 0.5;

- d (1×1) is a constant value defines the start point of sine function along the vertical axis, practically defined on the basis of geometric pattern comparison between the experimental curve of GRF along each axis and a typical sine curve which is equal to 0.5;

4.4.3.3 Computation of the sigmoid and sine-sigmoid functions

To compute GRF applying the sigmoid function, due to the pattern of the GRF during DS, we added the sine function to the first part of sigmoid function. Typical sigmoid functions start with a horizontal asymptote, however the GRF starts with an arch pattern. Therefore the first part (x_0 to Q) is combination of sine and sigmoid functions and the rest (Q to x_L) is fitted by only sigmoid function. Equations 14-16 show the calculation of sigmoid and sine-sigmoid functions' parameters used to compute GRF. All of the equations were defined based on the kinetic parameters during SS1 and SS2 provided by force platforms:

$$f(x) = \begin{cases} S_1(x) + S_2(x) & \text{for } \frac{|dS(x)|}{|dx|} > L \\ S_1(x) & \text{for } \frac{|dS(x)|}{|dx|} \leq L \end{cases} \quad (14)$$

$$S_1(x) = \frac{A_{sig}}{1 + e^{B_{sig}(x - C_{sig})}} \tag{15}$$

$$S_2(x) = \begin{cases} \frac{dFSS \times t_c}{8} \times \sin\frac{\pi(x - x_0)}{t_c} & \text{ML and AP GRF} \\ \frac{dFSS \times t_c}{8} \times \sin\frac{\frac{\pi}{2}(x - x_0) - \frac{\pi}{2}}{t_c} & \text{V GRF} \end{cases} \tag{16}$$

$$f(x) = \begin{cases} S_1(x) + S_2(x) & \text{for } \frac{|dS(x)|}{|dx|} > L \\ S_1(x) & \text{for } \frac{|dS(x)|}{|dx|} \leq L \end{cases} \tag{17}$$

where

- $S_1(x)$ is a sigmoid function;

- $S_2(x)$ is a sine function;

- $\frac{dS_1(x)}{dx}$ is the derivative of the sigmoid function;

- L (1×1) is a constant value obtained practically based on geometric pattern comparison between the experimental curve of GRF along each axis and a typical sigmoid curve, equal to 0.01 for ML, 2.4 for AP and 6.5 for V GRF. It defines the point where the added sine function to the sigmoid function should be terminated, whatever the value is bigger, the computed curve starts with bigger arc;

- Q (1×1) is the first time during DS where $\left|\frac{dS_1(x)}{dx}\right|$ is equal to L;

- A_{sig}(1×1) is the codomain of sigmoid function, which is equal to $LFSS$, value of the GRF in the last frame of SS1;

- B_{sig} (1×1) is a constant value obtained practically based on the geometric curve pattern.it defines the slope of sigmoid curve, as it increases the curve is steeper, which is 11.5 for AP and ML GRF and 6.5 for V GRF;

- $$C_{sig} = \begin{cases} x_0 + m \times t_{DS} + \dfrac{|dFSS_1|}{n} & \text{ML and AP GRF} \\ x_0 + m \times t_{DS} & \text{V GRF} \end{cases} \qquad (18)$$

- t_c (vector, n×1) is the time between x_0 and when $\dfrac{dS_1(x)}{dx} = L$;

- x_0 (1×1) is the last frame of the first SS before DS;

- $dFSS$ (1×1) is the slope of GRF in the last 5 frames SS1;

- m (1×1) is a constant value defining center of sigmoid function during DS, obtained practically based on the geometric pattern comparison between the experimental curve of GRF along each axis and a typical sigmoid curve which is 0.5 for ML and V GRF and 0.6 for AP GRF;

- n (1×1) is a constant value defining the horizontal phase shift of the sigmoid function, which is 4 for ML and 15 for AP GRF;

- s is equal to 3, defining the vertical shift of sine function of the fitted curve.

The GRF of the second foot that lands obtained by subtracting the GRF of the first foot from the total GRF and is obtained as follows (step 5):

$$F_{second\ foot} = F_{tot} - F_{computed} \qquad (19)$$

where,

- F_{tot} [N] is a vector (n×1) of total recorded GRF by force platforms;

- $F_{second\ foot}$ [N] is a vector (n×1) of GRF of second foot that lands;

$F_{computed}$ [N] is a Vector (n×1) of computed GRF of the first foot that lands.

4.5 GRF error analysis

During the DS, the mean absolute error e_F (1×1) between calculated and recorded GRF is defined as (step 6):

$$e_F = |F_{computed} - F_{measured}| \qquad (20)$$

where

- $F_{computed}$ [N] is a vector (n×1) of GRF computed by the proposed method;

- $F_{measured}$ [N] is a vector (n×1) of individually measured GRF on each platform during DS;
- n is a vector that defines the number of recorded samples during the DS.

Finally the best function fitted for each axis was chosen based on the minimal value of mean relative error (step 7).

Complementarily, a mean relative error ε_F (1×1) is defined as follow:

$$\varepsilon_F = \frac{e_F}{|F_{max}|} \qquad (21)$$

where,

- F_{max} (1×1) is maximal measured GRF during DS.

The mean global absolute and mean relative error of 3D-GRF were calculated with the chosen function for GRF along each axes, as bellow:

$$e_G = |F_{computed,G} - F_{measured,G}| \qquad (22)$$

where,

- e_G (1×1) is mean of global absolute error;

$$F_{computed,G} = \sqrt{F^2_{x,computed} + F^2_{y,computed} + F^2_{z,computed}} \qquad (23)$$

- $F_{computed,G}$ [N] is a vector (n×1) of computed 3D-GRF calculated by best function for each axis;

$$F_{measured,G} = \sqrt{F^2_{x,measured} + F^2_{y,measured} + F^2_{z,measured}} \qquad (24)$$

- $F_{measured,G}$ [N] is a vector (n×1) of independent recorded 3D-GRF by force platforms

$$\mathcal{E}_G = \frac{e_G}{|F_{G,max}|} \qquad (25)$$

- $\mathcal{E}_G$ (1×1) is the mean of global relative error

- $F_{G,max}$ (1×1) is the maximal 3D-GRF during DS phase

4.6 Results

Figures 4.3a-c illustrate the results of computed GRF for one subject using all the functions predicting the GRF vs. the actual recorded GRF.

4.3a.

4.3b.
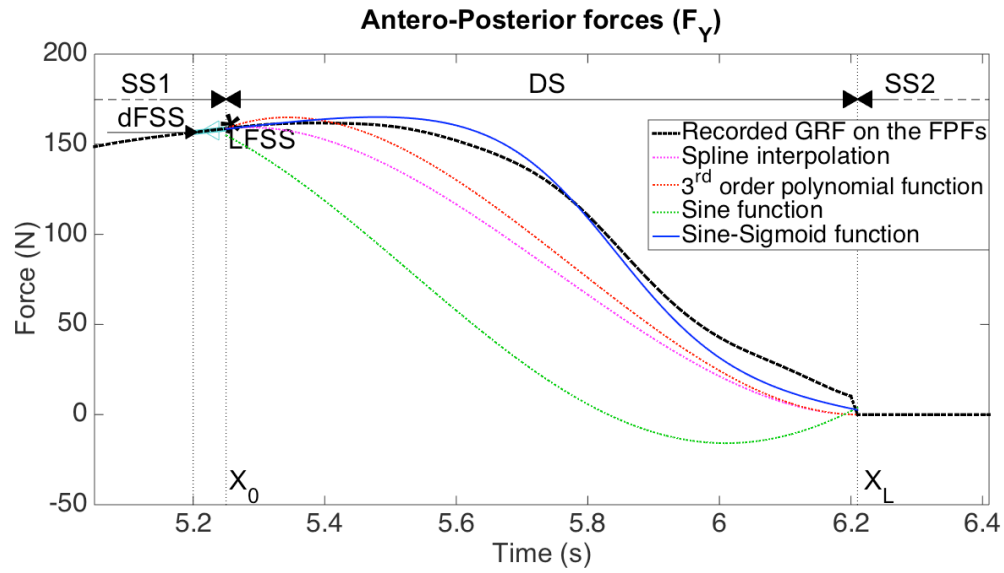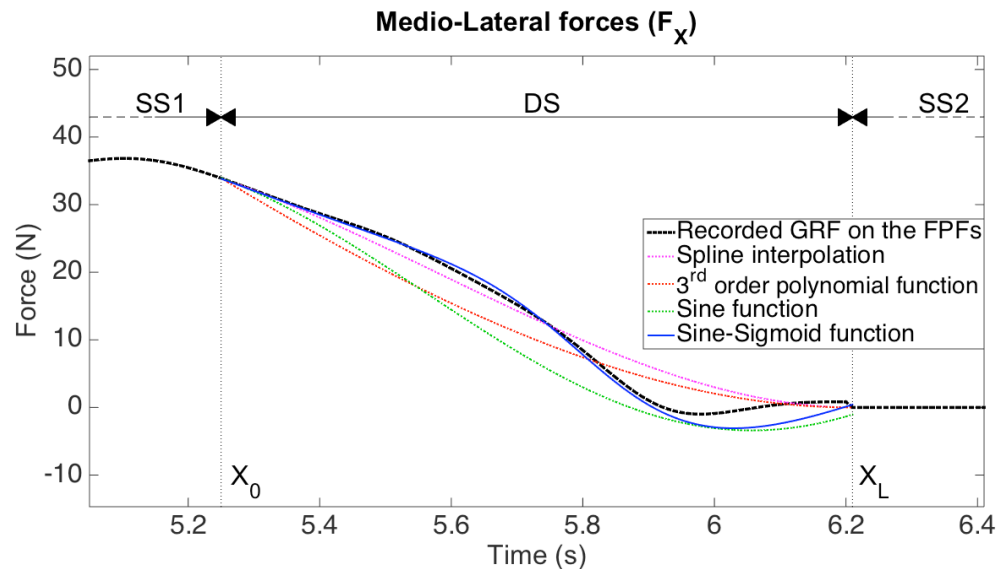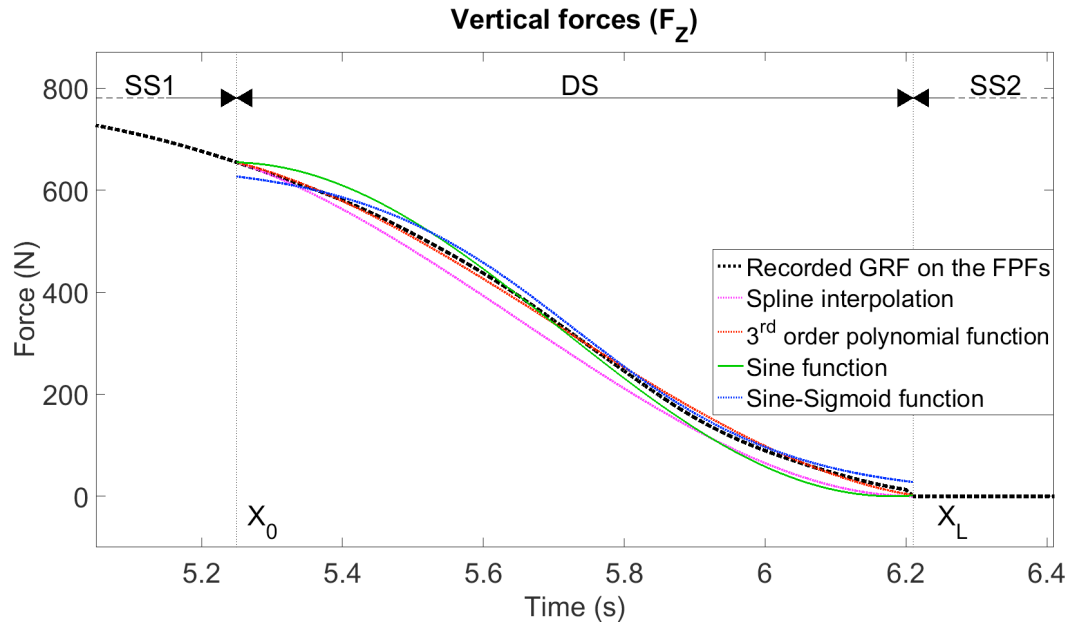
Vertical forces (F$_Z$)

4.3c.

Figure 4.3a: Antero-posterior (AP) forces during SS1, DS and SS2, b**.** Medio-lateral (ML) forces during SS1, DS and SS2, c. Vertical (V) forces during SS1, DS and SS2.

Recorded trial on the FPFs (black), spline interpolation (magenta), parametric curve modeling using sine function (cyan), parametric curve modeling using sigmoid-sine function (blue), parametric curve modeling using 3rd order polynomial function (red).

SS1: The first single stance phase before double stance, DS: Double stance phase, SS2: Second single stance phase after double stance,: Value of GRF in the last SS1 frame, Slope of GRF in the last 5 frames of SS1, x$_0$: Last frame of first single stance (SS) before double stance (DS), x$_L$: First frame of second SS after DS where the first foot leaves the floor, FPFs: Force platforms

Table 4.1 presents the mean relative errors and the mean absolute errors normalized by body mass between the computed and measured GRF. The mean relative error obtained from using the different functions does not vary greatly, which can leads us to think that the functions were indeed selected properly. The minimal mean relative error calculated for each force component is shown in underlined bold.

Table 4.1: Statistical results of the 30 participants.

ε_{mean}, e_{abs} , e_{max}, and e_{min}, respectively, mean relative error between computed and recorded ground reaction forces (GRF), mean absolute error between computed and recorded GRF normalized to body mass (BM), maximal and minimal absolute error. DS: Double stance; ML: Medio-lateral GRF (Fx); AP: Antero-posterior GRF (Fy); V: Vertical GRF (Fz)

Decomposed method	GRF	$\varepsilon_{mean}\pm SD$ (%)	$e_{abs}/BM\pm SD$ (N/Kg)	e_{max} (N)	e_{min} (N)
Spline interpolation [9]	ML	10.2 ± 4.9	0.07 ± 0.04	12.9	1.3
	AP	12.7 ± 6.5	0.3 ± 0.13	40.6	8.5
	V	3.3 ± 2.0	0.5 ± 0.33	94.1	12.1
3rd order Polynomial	ML	10.7 ± 4.6	0.1 ± 0.04	11.2	1.4
	AP	14.8 ± 8.6	0.4 ± 0. 2	61.6	8.8
	V	3.0 ± 2.0	0.4 ± 0.29	90.5	10.4
Sine	ML	9.9 ± 3.9	0.1 ± 0.04	13.4	1.2
	AP	10.7 ±5.7	0.3 ± 0.12	32.5	7.3
	V	**2.9 ±1.6**	0.4 ± 0.23	79.4	11.4
Sigmoid	ML	11.4 ± 5.1	0.1 ± 0.04	13.8	1.9
	AP	9.1 ± 4.9	0.2 ± 0.10	26.5	4.0
	V	3.1 ±1.7	0.4 ± 0.20	81.6	9.3
Sine-Sigmoid	**ML**	**9.5 ± 3.6**	0.1 ± 0.04	11.8	1.0
	AP	**6.6 ± 4.4**	0.2 ± 0.09	24.1	4.1
	V	3.3 ±1.7	0.5 ± 0.23	79.5	13.2

Table 4.1 mainly presents a low mean relative error of 2.9% (SD: 1.6%) for the vertical forces using the sine function, and the values of 6.6% (SD: 4.4%) and 9.5% (SD: 3.6%) for antero-posterior and medio-lateral forces respectively using the sine-sigmoid function, were reported. It provides the global 3D-GRF error equal to 3.2% (SD: 1.9%) on global GRF.

Table 4.2 reports the number of subjects, fitted with minimal value of error for each modeling function and spline interpolation to observe the most fitted function along each axis.

Table 4.2: Comparison of the number of subjects fitted with each method.

	Spline interpolation	Parametric curve fitting			
		3rd Order polynomial	Sigmoid	Sine	Sine-Sigmoid
ML GRF	5	0	1	14	10
AP GRF	5	0	4	2	19
V GRF	3	8	5	9	5

During one DS, the computation times were 0.4, 0.8, and 0.9 ms for V, AP, and ML GRF decompositions respectively during one double stance phase, compared to 60 ms using spline curve interpolation for V, AP and ML GRF.

4.7 Discussion

The current study proposed a new method to improve the accuracy of decomposition of GRF during double stance phase (DS) of gait using s-type parametric curve modeling.

Table 4.1 mainly presents a low mean relative error of 2.9% (SD: 1.6%) for the vertical forces using the sine function, and the values of 6.6% (SD: 4.4%) and 9.5% (SD: 3.6%) for antero-

posterior and medio-lateral forces respectively using the sine-sigmoid function, were reported. It provides the global 3D-GRF error equal to 3.2% (SD: 1.9%) on global GRF.

Observing the behavior of GRF during DS (Figure 4.3a-c, appendix 1a-c), shows that the vertical GRF, unlike the AP and ML GRF, almost follows similar geometric patterns among the different subjects. It can justify the interest of studies decomposing V GRF solely [8,9,18] in comparison to studies decomposing GRF along X and Y axes [21,22] and also the lower value of relative error compared to AP and ML GRF.

Table 4.2 reports the number of subjects, fitted with minimal value of error for each modeling function and spline interpolation to observe the most fitted function along each axis.

Comparing our results with the cited ones, one can notice an increase up to 47% and 38% of mean relative errors in decomposition of ML and V GRF respectively proposed in [9,21,22]. We could also obtain maximum GRF difference normalized to body mass lower than 1 N/kg (0.1 N/kg, 0.1 N/kg, 0.9 N/kg, for AP, ML and V respectively) which is equivalent to the results presented in Villeger et. al [22].

Finally, the process works in real-time, enabling to be implemented on platform paths. Further, a translation of the code from MATLAB to a real-time dedicated process, e.g. in C++, would certainly reduce this time by a factor of 100.

The proposed decomposition method and the phase detection procedure are sensitive to the noise, therefore a low-pass filter were applied to the data base. It can be considered as the limitation of the method while implementing on the other data base with higher value of noise.

4.8 Conclusion

This study proposed an automatic 3D-GRF decomposition method during gait, tested on 30 subjects. The global error on the GRF, i.e. 3.2±1.9%, was obtained using sine-sigmoid function for AP and ML GRF, and sine function for V GRF. This error is the best one in the literature. Further, the process works in real-time, enabling to be implemented on platform paths. Consequently, the method is recommended to be implemented on devices to obtain the 3D-GRF on several gait cycles using platform paths, such as sensory floors [21,28] and treadmills [25] or conventional juxtaposed force platforms.

The perspectives are to validate the method for various populations with musculo-skeletal disorders, extend it to various movement analyses, such as gait with a cane or a walker, and compute the corresponding spatio-temporal parameters without the use of any motion capture system.

ACKNOWLEDGMENTS

REFERENCES

[1]   L.-N. Veilleux, M. Raison, F. Rauch, M. Robert, L. Ballaz, Agreement of spatio-temporal gait parameters between a vertical ground reaction force decomposition algorithm and a motion capture system, Gait Posture. 43 (2016) 257–264. doi:10.1016/j.gaitpost.2015.10.007.

[2]   C.H. Soo, J.M. Donelan, Coordination of push-off and collision determine the mechanical work of step-to-step transitions when isolated from human walking, Gait Posture. 35 (2012) 292–297. doi:10.1016/j.gaitpost.2011.09.102.

[3]   R. Kale Moyano, Human gait characterization using Kinect, (2015). http://repositori.upf.edu/handle/10230/25322 (accessed May 13, 2016).

[4]   S. Hernandez, M. Raison, A. Torres, G. Gaudet, S. Achiche, From on-body sensors to in-body data for health monitoring and medical robotics: A survey, in: 2014 Glob. Inf. Infrastruct. Netw. Symp. GIIS, 2014: pp. 1–5. doi:10.1109/GIIS.2014.6934279.

[5] V. Marconi, H. Hachez, A. Renders, P.-L. Docquier, C. Detrembleur, Mechanical work and energy consumption in children with cerebral palsy after single-event multilevel surgery, Gait Posture. 40 (2014) 633–639. doi:10.1016/j.gaitpost.2014.07.014.

[6] N. Amiryarahmadi, W. Kropp, K. Larsson, Application of LMS Algorithm to Measure Low-Frequency Transient Forces from Human Walking, Acta Acust. United Acust. 102 (2016) 23–34. doi:10.3813/AAA.918921.

[7] E. Oggero, G. Pagnacco, D.R. Morr, S.R. Simon, N. Berme, Probability of valid gait data acquisition using currently available force plates, Biomed. Sci. Instrum. 34 (1997) 392–397.

[8] B.L. Davis, P.R. Cavanagh, Decomposition of superimposed ground reaction forces into left and right force profiles, J. Biomech. 26 (1993) 593–597.

[9] L. Ballaz, M. Raison, C. Detrembleur, Decomposition of the vertical ground reaction forces during gait on a single force plate, J. Musculoskelet. Neuronal Interact. 13 (2013) 236–243.

[10] P.E. Martin, A.P. Marsh, Step length and frequency effects on ground reaction forces during walking, J. Biomech. 25 (1992) 1237–1239.

[11] D. Janssen, W.I. Schöllhorn, K.M. Newell, J.M. Jäger, F. Rost, K. Vehof, Diagnosing fatigue in gait patterns by support vector machines and self-organizing maps, Hum. Mov. Sci. 30 (2011) 966–975. doi:10.1016/j.humov.2010.08.010.

[12] X. Qu, J.C. Yeo, Effects of load carriage and fatigue on gait characteristics, J. Biomech. 44 (2011) 1259–1263. doi:10.1016/j.jbiomech.2011.02.016.

[13] T. Marasovic, M. Cecic, V. Zanchi, Analysis and Interpretation of Ground Reaction Forces in Normal Gait, WTOS. 8 (2009) 1105–1114.

[14] F. Martínez-Martí, M.S. Martínez-García, S.G. García-Díaz, J. García-Jiménez, A.J. Palma, M.A. Carvajal, Embedded sensor insole for wireless measurement of gait parameters, Australas. Phys. Eng. Sci. Med. Support. Australas. Coll. Phys. Sci. Med. Australas. Assoc. Phys. Sci. Med. 37 (2014) 25–35. doi:10.1007/s13246-013-0236-7.

[15] L.N. Veilleux, M. Robert, L. Ballaz, M. Lemay, F. Rauch, Gait analysis using a force-measuring gangway: intrasession repeatability in healthy adults, J. Musculoskelet. Neuronal Interact. 11 (2011) 27–33.

[16] G.M. Meurisse, F. Dierick, B. Schepens, G.J. Bastien, Determination of the vertical ground reaction forces acting upon individual limbs during healthy and clinical gait, Gait Posture. 43 (2016) 245–250. doi:10.1016/j.gaitpost.2015.10.005.

[17] B. Samadi, M. Raison, C. Detrembleur, L. Ballaz, Real-time detection of reaction forces during gait on a ground equipped with a large force platform, in: 2014 Glob. Inf. Infrastruct. Netw. Symp. GIIS, 2014: pp. 1–3. doi:10.1109/GIIS.2014.6934268.

[18] H. Hijazi, H.E. Makssoud, Modeling of vertical ground reaction forces during double stance phase of the gait cycle for real-time treadmill measurements, in: 2015 Int. Conf. Adv. Biomed. Eng. ICABME, 2015: pp. 238–241. doi:10.1109/ICABME.2015.7323296.

[19] M. Yazji, M. Raison, C.-É. Aubin, H. Labelle, C. Detrembleur, P. Mahaudens, M. Mousny, Are the mediolateral joint forces in the lower limbs different between scoliotic and healthy subjects during gait?, Scoliosis. 10 (2015) S3. doi:10.1186/1748-7161-10-S2-S3.

[20] L. Ren, R.K. Jones, D. Howard, Whole body inverse dynamics over a complete gait cycle based only on measured kinematics, J. Biomech. 41 (2008) 2750–2759. doi:10.1016/j.jbiomech.2008.06.001.

[21] S.E. Oh, A. Choi, J.H. Mun, Prediction of ground reaction forces during gait based on kinematics and a neural network model, J. Biomech. 46 (2013) 2372–2380. doi:10.1016/j.jbiomech.2013.07.036.

[22] D. Villeger, A. Costes, B. Watier, P. Moretto, An algorithm to decompose ground reaction forces and moments from a single force platform in walking gait, Med. Eng. Phys. 36 (2014) 1530–1535. doi:10.1016/j.medengphy.2014.08.002.

[23] J.A. Zeni, J.G. Richards, J.S. Higginson, Two simple methods for determining gait events during treadmill and overground walking using kinematic data, Gait Posture. 27 (2008) 710–714. doi:10.1016/j.gaitpost.2007.07.007.

[24] C.M. O'Connor, S.K. Thorpe, M.J. O'Malley, C.L. Vaughan, Automatic detection of gait events using kinematic data, Gait Posture. 25 (2007) 469–474. doi:10.1016/j.gaitpost.2006.05.016.

[25] J.K.D. Witt, Determination of toe-off event time during treadmill locomotion using kinematic data, J. Biomech. 43 (2010) 3067–3069. doi:10.1016/j.jbiomech.2010.07.009.

[26] R.M. Kiss, Comparison between kinematic and ground reaction force techniques for determining gait events during treadmill walking at different walking speeds, Med. Eng. Phys. 32 (2010) 662–667. doi:10.1016/j.medengphy.2010.02.012.

[27] M. Rio, F. Colas, M. Andries, F. Charpillet, Probabilistic sensor data processing for robot localization on load-sensing floors, in: 2016. https://hal.inria.fr/hal-01274696/document (accessed May 15, 2016).

[28] M. Andries, Object and human tracking, and robot control through a load sensing floor, phdthesis, Université de Lorraine, 2015. https://hal.inria.fr/tel-01252938/document (accessed May 13, 2016).

[29] U. Lugrís, J. Carlín, R. Pàmies-Vilà, J.M. Font-Llagunes, J. Cuadrado, Solution methods for the double-support indeterminacy in human gait, Multibody Syst. Dyn. 30 (2013) 247–263. doi:10.1007/s11044-013-9363-x.

CHAPTER 5   METHODS

Complementarily to the method described in the paper (chapter 5), this chapter aims to present the methodology of the project precisely.

5.1 Experiments

5.1.1 Participants

To validate the proposed method on the subjects, experimental data were gathered. An experimental protocol for gait data acquisition in adults was defined and approved by the ethics committee of the Sainte-Justine Hospital Research Center.

33 healthy adults volunteered to participate in this project. Exclusion criteria for the participants with typical development were flatfoot, known orthopedic surgical and injuries during the last 2 years on the lower limb. The trials of 3 subjects were rejected. Two ones due to their unusual gait patterns, i.e. their toes landed before their hills and one because of having difficulty in achieving valid cycles, with both feet inside the force platforms. The final 30 participants had a mean age of 24.8 (SD: 3.1) years, ranged 20-34, consisting of 17 males and a mean weight of 70.6 (SD: 11.4) kg. The participants of the current study would be considered as a control group in the future studies on the clinical population. Thus the number of 30 individuals can be justified as a sufficient number for a control group.

5.1.2 Equipment set-up

Kinematics and kinetics: The process of collecting participant data was carried out in the motion laboratory of research Centre of Marie-Enfant rehabilitation center, equipped by a 3D motion capture system composed of 12 T40S cameras (*Vicon*, UK) cadenced at 100Hz and by three separate FPFs 50 x 50 cm^2) (*AMTI*, USA) embedded in the floor to record ground reaction forces at a frequency of 1000Hz (Figure 4.1). 33 reflective markers placed over several anatomic landmarks according to the full body plug in gait kinematic model were tracked (Figure 4.2).

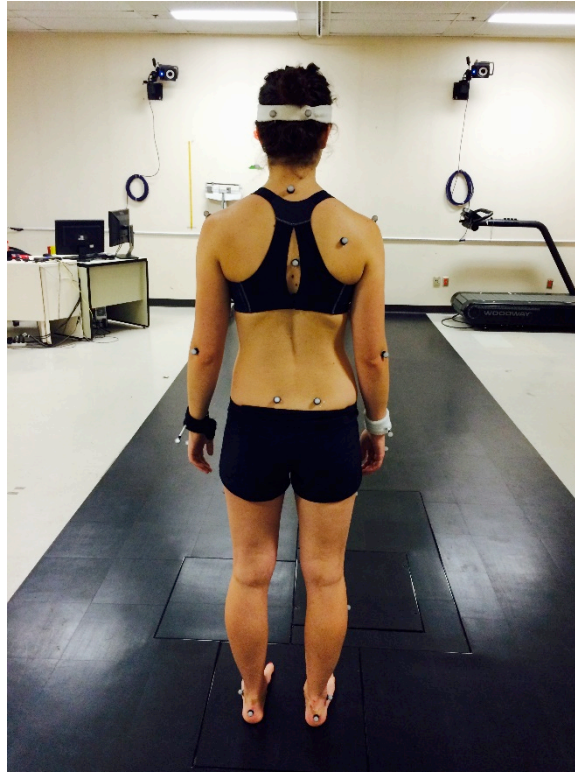Figure 5.1: Motion analysis laboratory

Figure 5.2: A participant performing the experiment

5.1.3 Procedure of data collection

The experimental procedure was explained for each participant and all participants provided written consent prior to test that has been approved by the ethics committee of the Sainte-Justine Hospital Research Center. The participants were asked to walk naturally barefoot at their own preferred pace, looking straight ahead without targeting their steps to obtain the valid cycles on the platforms. [7]. The trials with both steps inside the force platforms were used for this study. The motive behind this design was to easily record forces during untargeted stances in the walkway, enabling us to obtain independent left-right GRF. The recorded GRF during SS before and after DS were exported to be used in proposed method. To remove the noise, a low-pass filter with a 4th order Butterworth using 4Hz cut-off frequency was applied to the GRF.

5.1.4 Computed parameters and GRF decomposition procedure

The proposed method focuses on optimizing mathematical functions and GRF along each axis. For this purpose, the behavior of geometric curve pattern of the experimental GRF of 30 subjects including in the research project during DS, were compared with the typical behavior of different

mathematical functions i.e. S-curve, polynomial, rational, exponential, hyperbolic and periodic functions, using MATLAB® (Mathworks, Natick, Massachusetts, U.S.A) non-linear least squares (*lsqnonlin*) toolbox. *Lsqnonlin* solves nonlinear least-squares (nonlinear data-fitting) problems. Therefore 3rd order polynomial, sine and sigmoid functions that yielded the lowest error based on the studies performed as Integrator Project (PI3) by two undergraduate students in our laboratory, were selected as more appropriate functions to decompose 3D-GRF.During the integration of the different functions to decompose the GRF, it was noticed that the combination of sine and sigmoid function yielded better results for decomposing GRF in comparison to the sigmoid function solely (see chapter 4), therefore the sine-sigmoid function was applied.

Then the parameters of each function, used in decomposition GRF, were defined on the basis of kinetics parameters of gait during SS. The decomposed GRF of the foot, first landed, was obtained by defining each function parameters. It is worth noting that due to the different behavior of the proposed functions, the method of computing their parameters differs. To compute the parameters of 3rd order polynomial function, four simple equations based on the value of function and its derivative in the beginning and end of DS were defined and solved (see chapter 4). However, to compute the parameters of sine and sine-sigmoid functions, codomain, period, horizontal and vertical shift were used (see chapter 4).

Decomposed GRF of the second landed foot, was simply computed by subtracting the decomposed GRF of the first landed foot and total GRF, recorded by force platforms. To validate the method, the decomposed GRF were compared with the GRF recorded by force platforms to select the best function along X, Y and Z axes. Finally, the decomposed GRF, using parametric curve fitting model, were compared with the decomposed GRF using cubic spline method proposed by Ballaz *et al*. [7].

The equations used for decomposition GRF, computing error and selecting the best function for GRF along each axis have been briefly explained in the article presented in chapter 4.

CHAPTER 6   RESULTS

The results have been comprehensively presented in chapter 4. In this chapter, first the variety of geometric curve patterns of 3D-GRF are discussed, to give an idea about minimal and maximal errors reported in the presented article. Then the obtained results are compared to the results of the studies presented in chapter 2.

6.1 Observation on GRF during double stance phase

6.1.1 Observation on vertical (Fz) forces

Generally the V GRF at the beginning of DS is a continuation of a peak that occurring during SS. That peak is due to the push-off since the plantar flexors muscles are active, and finally it drops to zero as the opposite limb takes up the body weight [13]. Observing recorded V GRF showed that V GRF's curves have similar geometric patterns among all of the subjects.

6.1.2 Observation on antero-posterior (Fy) forces

Observing the general curve pattern of antero-posterior (AP) GRF, shows that there is a hump in DS and then it continues till it reaches to zero value, at the end of DS, where the foot leaves the ground. Due to the different walking behavior of each individual, it was noticed that for 73% of subjects, the hump reaches its peak in the first half part of the DS (Fig. 6.1 top), and for 27% of them, the AP curve reaches its peak during the second half part of DS (Fig. 6.1 bottom). Meanwhile, there are also some differences observing the general curve pattern of AP GRF, while the foot is near to takeoff. In some individuals (43%) the AP curve drops to zero by an almost horizontal asymptote (Fig. 6.1 top), while for the rest of the subjects (57%) (Fig. 6.1 bottom) the AP curves drop to zero with a certain slope.

Figure 6.1: Antero-posterior GRF during DS of two different individuals

SS1 : Single stance phase before double stance phase; DS : Double stance phase

6.1.3 Observations on Medio-lateral (Fx) forces

Medio-lateral (ML) GRF during DS are the continuation of a peak that has happened in SS, i.e. at the beginning of DS, ML GRF continue to maintain a decreasing slope, however in some (50%) (Fig. 6.2. top), ML GRF drops to zero with a decreasing slope from the peak, and in others (50%) (Fig. 6.2. bottom) the algebraic sign changes at the beginning of the DS and finally ML GRF drops in zero.
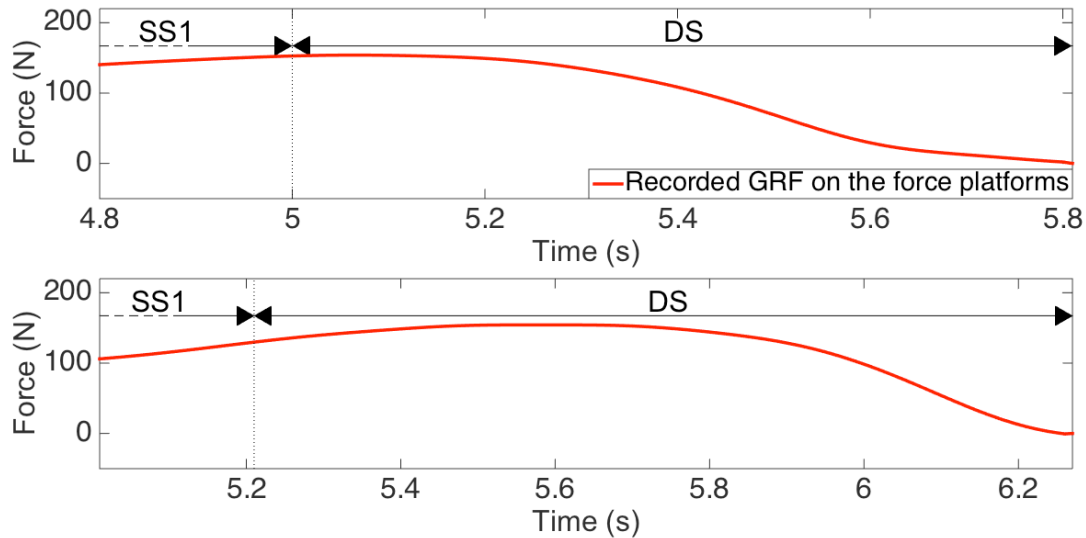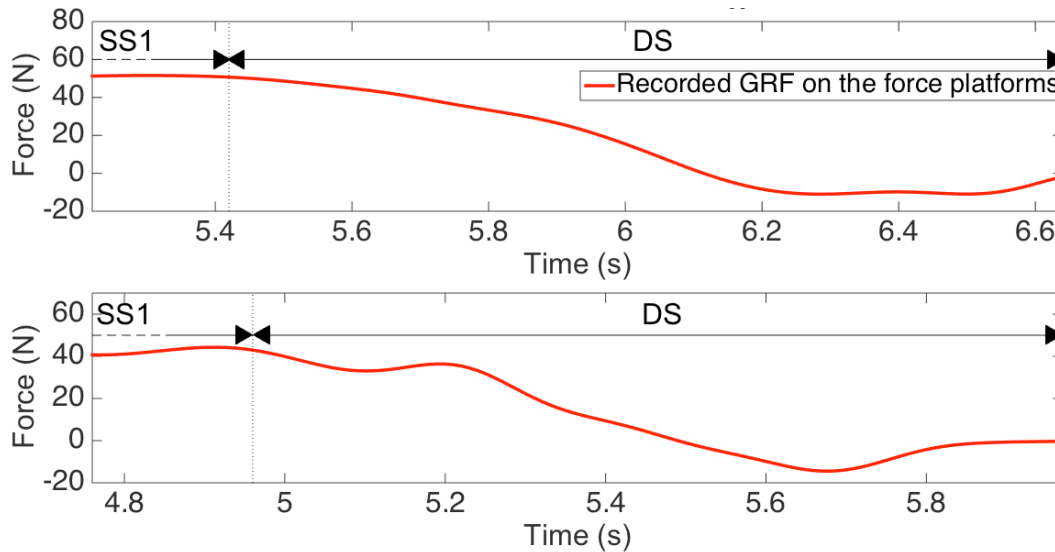
Figure 6.2: Medio-lateral GRF during DS of two different individuals

SS1 : Single stance phase before double stance phase; DS : Double stance phase

Consequently, observation of recorded GRFs along each axis, (V, AP and ML) showed that unlike the other axes, there is not any significant difference among the V GRF curves of all of the subjects. Due to this fact, the accuracy of decomposition methods is higher on V GRF in comparison to the AP and ML GRF.

6.2 Observation on the results

6.2.1 The mean relative error using s-type curve fitting model and spline cubic interpolation

The spline interpolation model was applied to decompose the 3D-GRF and the results in compare with s-type parametric curves model, are presented in table 6.1.

Table 6.1: Comparison of mean relative error using parametric curve fitting model and spline interpolation model to decompose 3D-GRF

	Mean relative error		
	V GRF	**AP GRF**	**ML GRF**
Spline interpolation model	3.3%	12.7%	10.2%
Parametric curve fitting model	2.9% (sine function)	6.6% (sine-sigmoid function)	9.9% (sine-sigmoid function)
Decrease of mean relative error using parametric curve fitting model	12.1%	48.0%	6.9%

6.2.2 Duration of 3D-GRF decomposition

Table 6.2 shows the duration of applying each model to decompose each GRF.

Table 6.2: Duration of 3D-GRF decomposition procedure using different models

Models	**Mean time (microseconds)**		
	V GRF	**AP GRF**	**ML GRF**
Spline interpolation model	60	60	60
3rd order Polynomial	0.03	0.05	0.05
Sine	0.4	0.4	0.5
Sine-sigmoid	0.04	0.8	0.9

6.2.3 Comparison of the results with the literature

To compare the results with the performed studies presented in chapter 2, table 6.3 shows the mean relative error of GRF decomposition.

Table 6.3: Comparison of the results among methods

Mean relative error computed from each decomposition method (%)				
GRF components	Oh et al.	Villeger et al.	Ballaz et al.	Current study
ML GRF	11,7	18,0	N.A.	9,6
Reduction to our method (%)	18	47	N.A.	
V GRF	4,7	3,8	3,8	2,9
Reduction to our method (%)	38	24	24	

CHAPTER 7   GENERAL DISCUSSION

Due to the wide range of interest in studying human gait, recording GRF during walking is needed in various domains. However, as explained in chapter 2, among the different set-up systems for recording GRF, using unique long force platforms is highly in demand [33]. The main challenge in using these long force platforms is obtaining the separated GRF under each foot. Therefore by using a unique long force platform, the need of applying an accurate decomposition method that can be simply implemented in various populations, such as children, adults, etc. is raised.

This study intended to develop an innovative method to improve the accuracy of decomposing 3D-GRF to both left and right profiles, during DS of the gait. To the author's best knowledge, no 3D-GRF decomposition method has been reported in the literature that was proposed without the use of motion capture system. Consequently, no method has been also validated on a large number of participants.

This chapter is divided into two sections: 1. Discussion on procedures and methods to compute the parameters of the functions; 2. The limits of the proposed method.

7.1 Discussion on procedures and methods to compute the parameters of the functions

As mentioned in 4.1.4, different methods were applied to compute the parameters of each function to obtain the decomposed GRF. In fact, computing the function parameters by using the value of the function and its derivative at the beginning and at the end of the DS provides the decomposed GRF for 3rd order polynomial function only. Meanwhile, due to the properties of sine and sine-sigmoid functions, using the mentioned method to compute the parameters lead to multiple answers for each parameter, and cannot provide a decomposed GRF similar to the recorded GRF. Therefore, for these functions, the parameters were defined on the basis of adjusting the geometric curve pattern of GRF during DS to the required part of the functions, by defining the period, codomain, horizontal and vertical shift of the functions. Kinetics parameters during SS before the DS were used to define period, codomain, horizontal and vertical shift.

It is worth noting that comprehensive studies were carried out on using hyperbolic tangent, arctangent and hyperbolic sine to decompose 3D-GRF. To compute the parameters of these mentioned functions, our proposed method (see chapter 4) could not be implemented because of the properties of the functions. Therefore optimization tools were needed to compute the parameters. We used MATLAB® and C^{++} (C^{++} Foundation) to estimate the parameters by iteration procedure. The initial value were needed for the parameters in optimization tools, as mentioned in the study performed by Hijazi and Makssoud (2015) [25]. The function parameters are very sensitive to the quality of initial values. Therefore, the optimization method could not be considered as a possible automatic method. However the presented sigmoid function has the similar curve pattern as hyperbolic tangent, arctangent and hyperbolic sine functions and the parameters can be calculated without the need for optimization procedure or solving any nonlinear least-squares problems (see chapter 4).

This proposed method can be applied on various clinical populations and functional rehabilitation evaluation, providing the mean relative error in the range of reported minimal and maximal mean relative error among 30 subjects.

7.2 The limits of the proposed method

The proposed method is sensitive to noises, therefore a low-pass filter was applied to remove noises. Implementing the method applying the same cut-off frequency as ours on the experimental data with higher value of noises than our recorded experimental data may lead to the higher value of the mean relative error. However in some cases, phase detection may not be performed properly without removing noise if the value of noise is close or higher than the value of peak of, which is the tool to detect phase transition.

Another limitation is the variety of the walking behavior in the individuals. Although the GRF in the healthy participants generally follow the same patterns, but the GRF are affected by position and motion of all body segments such as head, arms, trunk, pelvis and legs [13], as discussed in chapter 6. Classification of gait pattern of the individuals can be leaded to the more accurate results. We tried to categorize the gait pattern of the individuals using kinetic parameters during single stance phases, unfortunately kinetic parameters could not provide us a tool to classify the gait patterns.

In terms of choosing the functions, they were chosen by the preliminary studies using curve fitting tools to find the best functions. However the number of the functions can be considered as limited numbers since they were chosen by the user. The accuracy of the method can be improved if the functions can be selected automatically among numerous numbers of functions.

CHAPTER 8   CONCLUSION AND RECOMMENDATIONS

The objective of the project was to propose an automatic method in real-time to decompose three-dimensional ground reaction forces (3D-GRF) to the left and right profiles, along with the three axes of X, Y and Z during double stance phase of the gait. To develop this method, a parametric curve fitting model using kinetic parameters were applied, and the best fitted function for ground reaction forces (GRF) along each axis was chosen on the basis of comparing decomposed GRF with the individually recorded GRF by force platforms. The method was tested and validated on 30 healthy subjects (age: 24.8 (SD: 3.1) years, 17 male, weight: 70.6 (SD: 11.4) kg. The mean relative errors calculated by the proposed method, were also compared with the related mean relative errors applying spline curve interpolation proposed by Ballaz et al. (2013) [7]. The decomposed GRF obtained from the best function using curve-fitting model is more accurate compared to the decomposed GRF obtained from spline interpolation model. It can be justified, as spline interpolations do not consider the typical patterns of GRF, therefore they potentially are led to inaccuracies [21]. However, as presented in table 6.2, the duration of GRF decomposition during DS is reasonable and lower than the one obtained by the spline interpolation method.

The best function for antero-posterior (AP) and Medio-lateral (ML) GRF was sine-sigmoid and for vertical (V) was sine, with the mean relative error of 6.6% (SD: 4.4%), 9.5% (SD: 3.6%) and 2.9% (SD: 1.6%), respectively, and the global mean relative error based on the selected functions was 3.2% (SD: 1.9%). It shows that to minimize the error predicting 3D- GRF along each axis, one unique function cannot be used.

The current method proposed the decomposed vertical and medio-lateral GRF replicating more accurately the recorded GRF in comparison with the other studies, as shown in table 6.3.

In conclusion, this method is the first automatic method to decompose 3D-GRF independent of the motion capture systems, which can limit the application of the other existing decomposing methods.

As perspective, more studies are needed to be performed to implement the method in populations with musculoskeletal disorders and integrate in real-time. It can be also applied to long single force platforms performing several double stances. These can lead to the more convenient gait evaluation in this clinical population and eventually provide the use of the proposed method for functional evaluation in rehabilitation.

Furthermore, another venue would be to implant genetic programming to automatically evolve possible functions from experimental data.

BIBLIOGRAPHY

[1] L.-N. Veilleux, M. Raison, F. Rauch, M. Robert, and L. Ballaz, "Agreement of spatio-temporal gait parameters between a vertical ground reaction force decomposition algorithm and a motion capture system," *Gait Posture*, vol. 43, pp. 257–264, Jan. 2016.

[2] R. Headon and R. Curwen, "Recognizing Movements from the Ground Reaction Force," in *Proceedings of the 2001 Workshop on Perceptive User Interfaces*, New York, NY, USA, 2001, pp. 1–8.

[3] N. Amiryarahmadi, W. Kropp, and K. Larsson, "Application of LMS Algorithm to Measure Low-Frequency Transient Forces from Human Walking," *Acta Acust. United Acust.*, vol. 102, no. 1, pp. 23–34, Jan. 2016.

[4] E. Oggero, G. Pagnacco, D. R. Morr, S. R. Simon, and N. Berme, "Probability of valid gait data acquisition using currently available force plates," *Biomed. Sci. Instrum.*, vol. 34, pp. 392–397, 1997.

[5] P. E. Martin and A. P. Marsh, "Step length and frequency effects on ground reaction forces during walking," *J. Biomech.*, vol. 25, no. 10, pp. 1237–1239, Oct. 1992.

[6] D. Janssen, W. I. Schöllhorn, K. M. Newell, J. M. Jäger, F. Rost, and K. Vehof, "Diagnosing fatigue in gait patterns by support vector machines and self-organizing maps," *Hum. Mov. Sci.*, vol. 30, no. 5, pp. 966–975, Oct. 2011.

[7] L. Ballaz, M. Raison, and C. Detrembleur, "Decomposition of the vertical ground reaction forces during gait on a single force plate," *J. Musculoskelet. Neuronal Interact.*, vol. 13, no. 2, pp. 236–243, Jun. 2013.

[8] B. L. Davis and P. R. Cavanagh, "Decomposition of superimposed ground reaction forces into left and right force profiles," *J. Biomech.*, vol. 26, no. 4–5, pp. 593–597, May 1993.

[9] "Gait Analysis: Normal and Pathological Function," *J. Sports Sci. Med.*, vol. 9, no. 2, p. 353, Jun. 2010.

[10] "Shin splints biomechanics." [Online]. Available: http://www.shin-splints.co.uk/shinbiomechanics.htm. [Accessed: 18-Jun-2016].

[11] D. A. Winter, *Biomechanics and Motor Control of Human Movement*. John Wiley & Sons, 2009.

[12] J. L. Lelas, G. J. Merriman, P. O. Riley, and D. C. Kerrigan, "Predicting peak kinematic and kinetic parameters from gait speed," *Gait Posture*, vol. 17, no. 2, pp. 106–112, Apr. 2003.

[13] T. Marasovic, M. Cecic, and V. Zanchi, "Analysis and Interpretation of Ground Reaction Forces in Normal Gait," *WTOS*, vol. 8, no. 9, pp. 1105–1114, Sep. 2009.

[14] R. K. Begg and S. M. Rahman, "A method for the reconstruction of ground reaction force-time characteristics during gait from force platform recordings of simultaneous foot falls," *IEEE Trans. Biomed. Eng.*, vol. 47, no. 4, pp. 547–551, Apr. 2000.

[15] C. M. O'Connor, S. K. Thorpe, M. J. O'Malley, and C. L. Vaughan, "Automatic detection of gait events using kinematic data," *Gait Posture*, vol. 25, no. 3, pp. 469–474, Mar. 2007.

[16] J. A. Zeni, J. G. Richards, and J. S. Higginson, "Two simple methods for determining gait events during treadmill and overground walking using kinematic data," *Gait Posture*, vol. 27, no. 4, pp. 710–714, May 2008.

[17] J. B. Dingwell, B. L. Davis, and D. M. Frazier, "Use of an instrumented treadmill for real-time gait symmetry evaluation and feedback in normal and trans-tibial amputee subjects," *Prosthet. Orthot. Int.*, vol. 20, no. 2, pp. 101–110, Aug. 1996.

[18] R. Kram, T. M. Griffin, J. M. Donelan, and Y. H. Chang, "Force treadmill for measuring vertical and horizontal ground reaction forces," *J. Appl. Physiol. Bethesda Md 1985*, vol. 85, no. 2, pp. 764–769, Aug. 1998.

[19] J. S. Gottschall and R. Kram, "Energy cost and muscular activity required for propulsion during walking," *J. Appl. Physiol. Bethesda Md 1985*, vol. 94, no. 5, pp. 1766–1772, May 2003.

[20] A. M. Grabowski, "Metabolic and biomechanical effects of velocity and weight support using a lower-body positive pressure device during walking," *Arch. Phys. Med. Rehabil.*, vol. 91, no. 6, pp. 951–957, Jun. 2010.

[21] G. M. Meurisse, F. Dierick, B. Schepens, and G. J. Bastien, "Determination of the vertical ground reaction forces acting upon individual limbs during healthy and clinical gait," *Gait Posture*, vol. 43, pp. 245–250, Jan. 2016.

[22] S. Mckinley and M. Levine, *Cubic Spline Interpolation*. .

[23] S. E. Oh, A. Choi, and J. H. Mun, "Prediction of ground reaction forces during gait based on kinematics and a neural network model," *J. Biomech.*, vol. 46, no. 14, pp. 2372–2380, Sep. 2013.

[24] D. Villeger, A. Costes, B. Watier, and P. Moretto, "An algorithm to decompose ground reaction forces and moments from a single force platform in walking gait," *Med. Eng. Phys.*, vol. 36, no. 11, pp. 1530–1535, Nov. 2014.

[25] H. Hijazi and H. E. Makssoud, "Modeling of vertical ground reaction forces during double stance phase of the gait cycle for real-time treadmill measurements," in *2015 International Conference on Advances in Biomedical Engineering (ICABME)*, 2015, pp. 238–241.

[26] R. Fletcher, *Practical Methods of Optimization; (2Nd Ed.)*. New York, NY, USA: Wiley-Interscience, 1987.

[27] L. Ren, R. K. Jones, and D. Howard, "Whole body inverse dynamics over a complete gait cycle based only on measured kinematics," *J. Biomech.*, vol. 41, no. 12, pp. 2750–2759, Aug. 2008.

[28] R. K. Begg and S. M. Rahman, "A method for the reconstruction of ground reaction force-time characteristics during gait from force platform recordings of simultaneous foot falls," *IEEE Trans. Biomed. Eng.*, vol. 47, no. 4, pp. 547–551, Apr. 2000.

[29] J. K. D. Witt, "Determination of toe-off event time during treadmill locomotion using kinematic data," *J. Biomech.*, vol. 43, no. 15, pp. 3067–3069, Nov. 2010.

[30] M. Roerdink, B. (H.) Coolen, B. (H.)E. Clairbois, C. J. C. Lamoth, and P. J. Beek, "Online gait event detection using a large force platform embedded in a treadmill," *J. Biomech.*, vol. 41, no. 12, pp. 2628–2632, Aug. 2008.

[31] S. J. Lee and J. Hidler, "Biomechanics of overground vs. treadmill walking in healthy individuals," *J. Appl. Physiol.*, vol. 104, no. 3, pp. 747–755, Mar. 2008.

[32] L. A. Ferrari and R. J. Defigueiredo, "Curves and Surfaces in Computer Vision and Graphics," presented at the Curves and Surfaces in Computer Vision and Graphics, 1990, vol. 1251.

[33] L. N. Veilleux, M. Robert, L. Ballaz, M. Lemay, and F. Rauch, "Gait analysis using a force-measuring gangway: intrasession repeatability in healthy adults," *J. Musculoskelet. Neuronal Interact.*, vol. 11, no. 1, pp. 27–33, Mar. 2011.
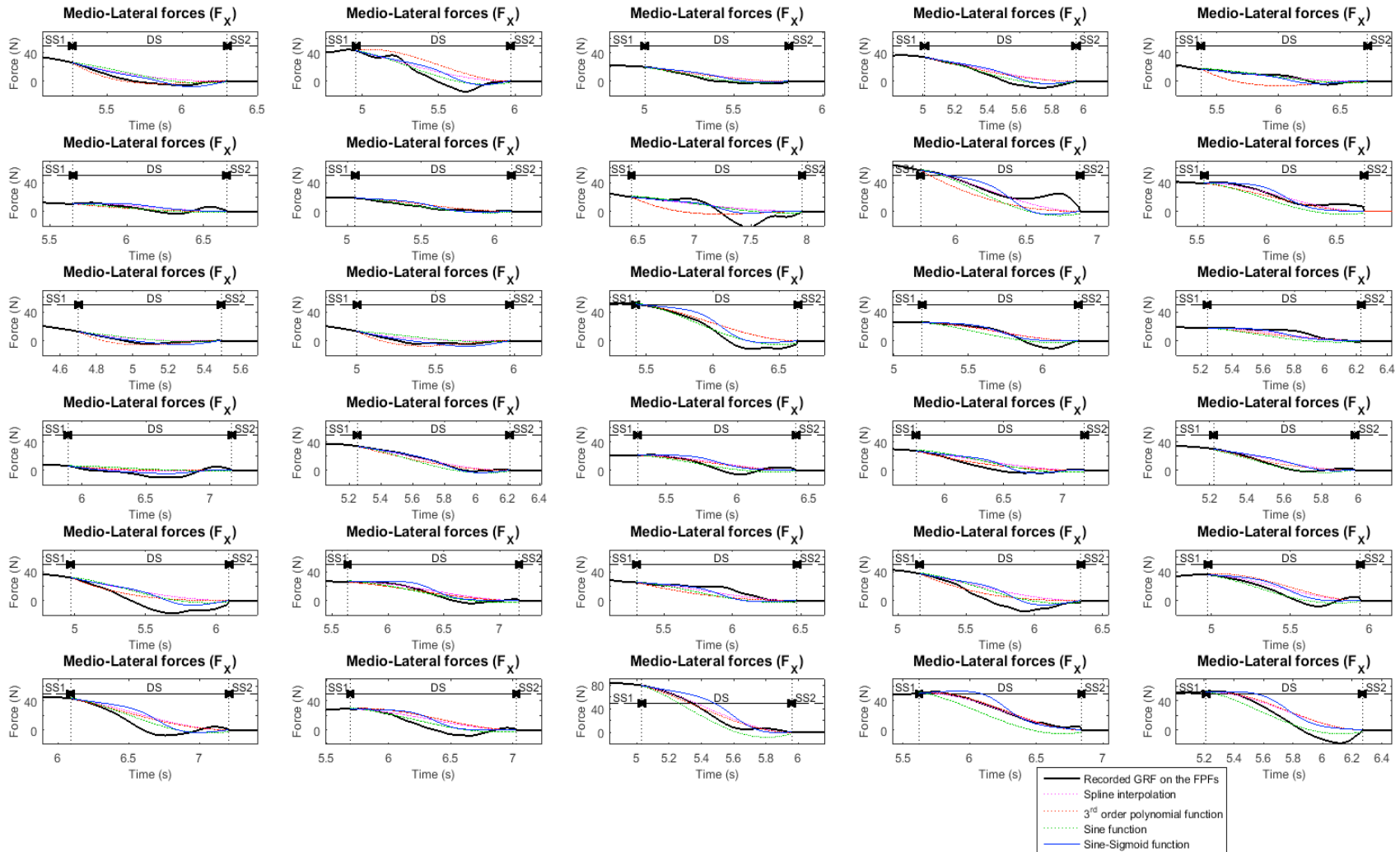
APPENDIX 1

Figure A.1.A – Medio-Lateral ground reaction forces for 30 subjects
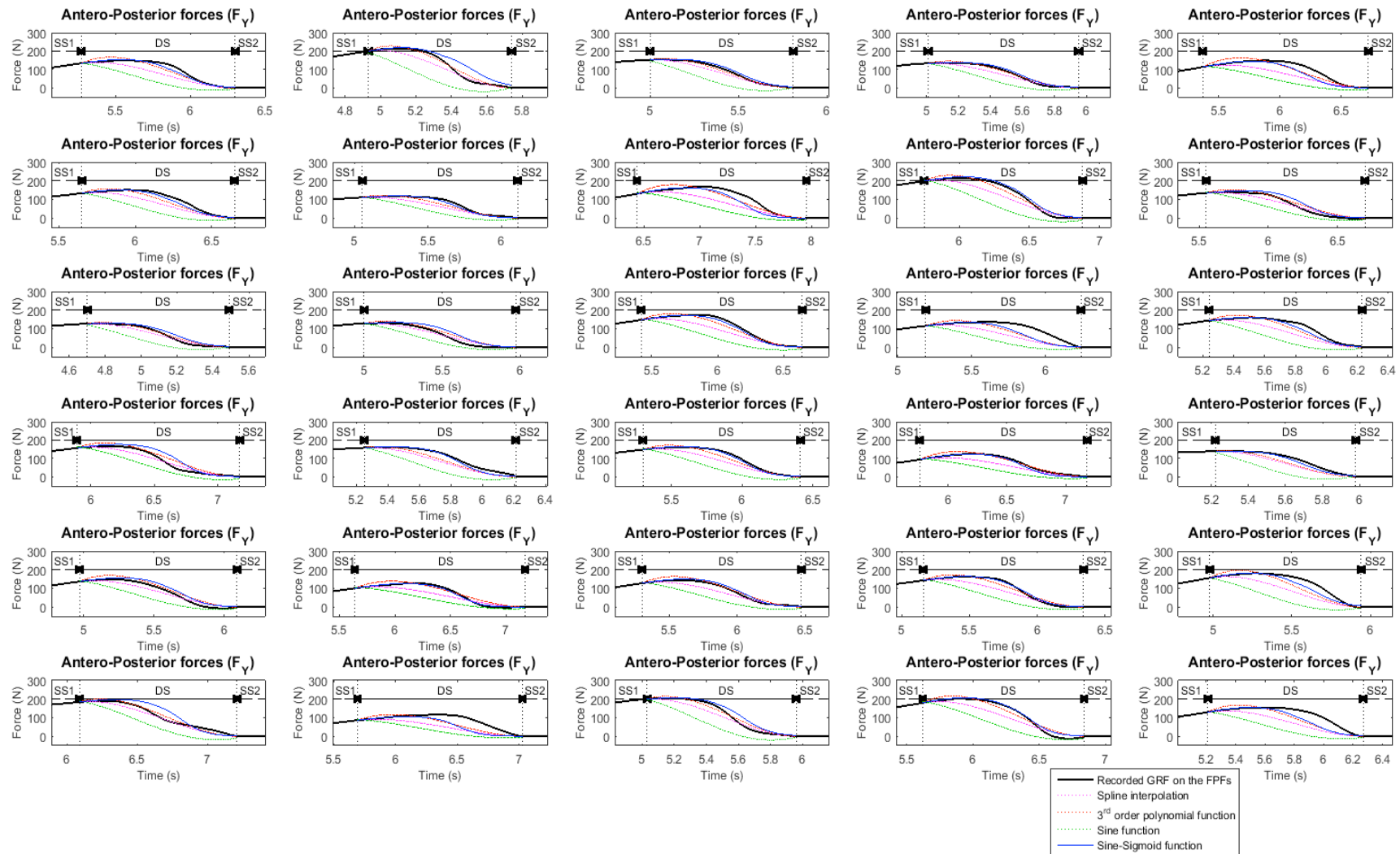
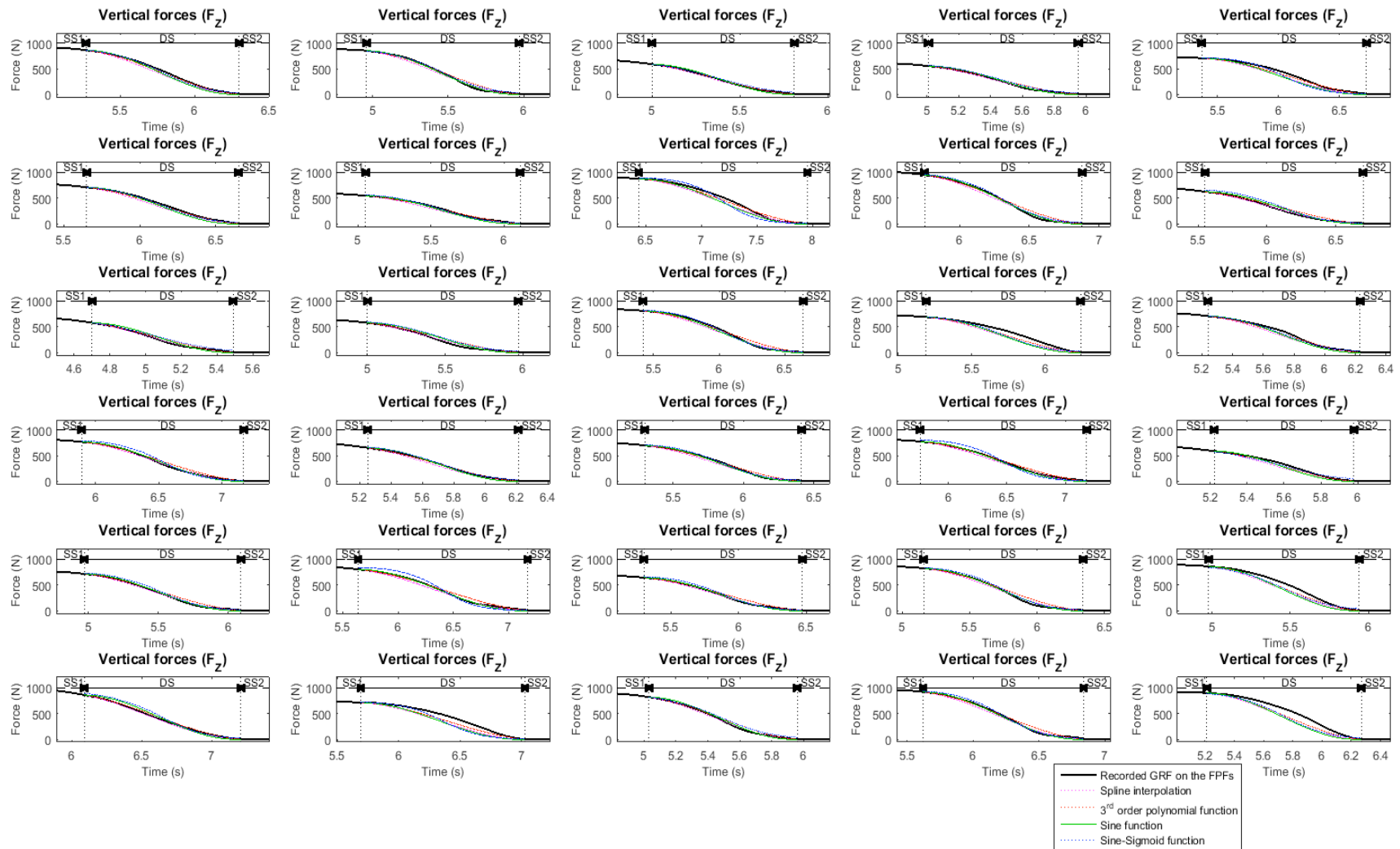Figure A.1.B – Antero-posterior ground reaction forces for 30 subjects

Figure A.1.C – Vertical ground reaction forces for 30 subjects